7-1-2022

Regulation of the Heat Shock Response via Lysine Acetyltransferase CBP-1 and in Neurodegenerative Disease in *Caenorhabditis elegans*

Lindsey N. Barrett
University of South Florida

Regulation of the Heat Shock Response via Lysine Acetyltransferase CBP-1 and in Neurodegenerative Disease in *Caenorhabditis elegans*

by

Lindsey N. Barrett

A dissertation submitted in partial fulfillment
of the requirements for the degree of
Doctor of Philosophy
with a concentration in Cellular and Molecular Biology
Department of Cell Biology, Microbiology, and Molecular Biology
College of Arts and Sciences
University of South Florida

Major Professor: Sandy D. Westerheide, Ph.D.
Meera Nanjundan, Ph.D.
Younghoon Kee, Ph.D.
Eric Guisbert, Ph.D.

Date of Approval:
July 1, 2022

Keywords: HSF-1, PTMs, aging, *C. elegans*

DEDICATION

I would like to dedicate this work to my sister, Whitney Snyder, who has given me endless love and advice. I would be nowhere without you. To my mother, Cheryl Snyder, for her continuous support and love. Thank you for always believing in me and supporting me especially through the roughest of times. To my mentor, Sandy D Westerheide. Thank you for your continual guidance and help in becoming a scientist. Thank you for allowing me the space to grow as a scientist and a person in your care. To my camping friends, who never stopped believing in me and filling my life with endless laughs and good times. You have kept me sane. You all are forever in my heart.

ACKNOWLEDGMENTS

I would like to acknowledge my committee members Dr. Meera Nanjundan, Dr. Younghoon Kee, and Dr. Eric Guisbert for the wonderful guidance and discussion throughout the years. I would also like to thank my colleagues Doreen Lugano, Andrew Deonarine, Veena Subramanian, and Vivek Somasundaram for your guidance and support throughout this journey.

TABLE OF CONTENTS

LIST OF TABLES

LIST OF FIGURES

LIST OF ACRONYMS

UPS – Ubiquitin-proteasome system
ALP – Autophagy-lysosome pathway
UPR – Unfolded protein response
ER – Endoplasmic reticulum
HSR – Heat shock response
HSF-1 – Heat shock transcription factor 1
HSP – Heat shock protein
HSE – Heat shock element
DBD – DNA binding domain
HR-A/B – Heptad repeats A/B
TAD – Transactivation domain
RD – Regulatory domain
PTM – post-translational modification
nSB – Nuclear stress body
KAT – Lysine acetyltransferase
SIRT1 – Sirtuin 1
CK2 – Casein kinase 2
NDD – Neurodegenerative disease
dsRNA – Double stranded RNA
RNAi – RNA interference
qPCR – quantitative polymerase chain reaction
EV – empty vector
Aβ – amyloid-beta
polyQ – polyglutamine
α-syn – alpha-synuclein
GFP – Green fluorescent protein
L1 – Larval stage 1
L2 – Larval stage 2
L3 – Larval stage 3
L4 – Larval stage 4

ABSTRACT

The decline of proteostasis is a hallmark of aging that is, in part, affected by the dysregulation of the heat shock response (HSR), a highly conserved cellular response to proteotoxic stress in the cell. The heat shock transcription factor HSF-1 is well-studied as a key regulator of proteostasis, but mechanisms that could be used to modulate HSF-1 function to enhance proteostasis during aging are largely unknown. In this study, we examined lysine acetyltransferase regulation of the HSR and HSF-1 in *C. elegans*. We performed an RNA interference screen of lysine acetyltransferases and examined mRNA expression of the heat-shock inducible gene *hsp-16.2*, a widely used marker for HSR activation. From this screen, we identified one acetyltransferase, CBP-1, the *C. elegans* homolog of mammalian CREB-binding protein CBP/p300, as a negative regulator of the HSR. We found that while knockdown of CBP-1 decreases the overall lifespan of the worm, it also enhances heat shock protein production upon heat shock and increases thermotolerance of the worm in an HSF-1 dependent manner. Similarly, we examined a hallmark of HSF-1 activation, the formation of nuclear stress bodies (nSBs). In analyzing the recovery rate of nSBs, we found that knockdown of CBP-1 enhanced the recovery and resolution of nSBs after stress. Collectively, our studies demonstrate a role of CBP-1 as a negative regulator of HSF-1 activity and its physiological effects at the organismal level upon stress.

Defects in proteostasis that occur with aging are also central to many human diseases, including Alzheimer's disease, Parkinson's disease, and Huntington's disease. These neurodegenerative diseases (NDDs) are proteotoxic diseases hallmarked by increased protein misfolding and aggregation. Many components of the heat shock response are downregulated in NDD and aging,

including HSF1. The regulation of HSF-1 in neurodegenerative diseases has yet to be fully elucidated. Thus, we examined regulation of HSF1 and its target genes in NDD models in *C. elegans.* We found that *hsf-1* expression is decreased in an Alzheimer's disease model expressing human amyloid-β1-42 (Aβ). In contrast, we found that the presence of Aβ increased the expression of heat shock inducible HSF-1 target genes *hsp-16.2* and *hsp-70*. To further examine the relationship between HSF-1 and Aβ, we utilized an endogenous HSF-1::GFP worm strain previously made in the lab that we then crossed with the Aβ model of Alzheimer's disease to visualize tissue-specific HSF-1 expression in the disease state and with age. We visualized HSF-1::GFP foci in multiple tissue types in the Aβ background. Collectively, these findings begin uncovering the regulation of HSF-1 and the heat shock response in neurodegenerative disease in *C. elegans*.

Lastly, the mechanism of HSF1 degradation in general, and in neurodegenerative disease in particular, is not thoroughly characterized. Recent studies have identified two E3 ubiquitin ligases, FBXW7 and NEDD4, that target HSF1 for degradation in Huntington's and Parkinson's disease, respectively. Our goal is to further elucidate the mechanism of HSF1 degradation in neurodegenerative disease using *C. elegans* models. We have found that knockdown of the *C. elegans* homologs for FBXW7 and NEDD4, *sel-10* and Y92H12A.2, does not alter HSP reporter, *hsp-16.2*p::GFP and *hsp-70*p::GFP, activity in the wildtype background. However, we also examined E3 ligase knockdown in a Huntington's disease model that expresses polyglutamine expansions with age. In this neurodegenerative disease background, we found that *sel-10* and Y92H12A.2 RNAi increased motility and thermotolerance. Thus, both E3 ligases only regulate the HSR in the presence of polyglutamine expansions. These studies provide more knowledge on the regulation of HSF-1 in neurodegenerative disease, specifically Huntington's disease, and a

potential mechanism for the decrease in HSR activity in the presence of proteotoxic aggregate formation.

CHAPTER ONE: INTRODUCTION

The Proteostasis Network and the Heat Shock Response

Protein homeostasis, or proteostasis, is the proper balance of protein folding, trafficking, and clearance in the cell (Labbadia & Morimoto, 2015). The proteostasis network is a multi-compartmental system that encompasses the entire protein life cycle, from protein synthesis and folding to protein disaggregation and degradation. The regulation of proteostasis is critical for cell survival and function (Labbadia & Morimoto, 2015). There are three highly linked branches of this network that maintain the proteome: protein synthesis and folding, protein maintenance, and protein degradation. This network is comprised of ~2,000 proteins in human cells that control and regulate these branches to ensure proper cell survival (Labbadia & Morimoto, 2015).

Protein synthesis and folding

The human proteome is highly complex, with each cell and tissue type having a unique and distinct composition of proteins (Kulak, Geyer, & Mann, 2017). Each protein also ranges significantly in their abundance, and this can also vary between cell types (Geiger, Wehner, Schaab, Cox, & Mann, 2012). Once a protein is synthesized, it must be folded into its native state in order to function properly. The native or folded state of the protein is generally thermodynamically favorable. Proteins are folded with the help of molecular chaperones, or proteins that interacts and stabilizes or aids in the folding of another protein without being a part of its final form (Y. E. Kim, Hipp, Bracher, Hayer-Hartl, & Hartl, 2013). Many molecular chaperones are also known as heat shock proteins, as they were discovered to be synthesized

upon stress and also aid in the refolding of proteins that are misfolded or aggregated after stress (Y. E. Kim et al., 2013). Maintaining proper folding of proteins is critical to their function and overall cell survival.

Protein degradation

In conjunction with protein synthesis and maintenance, regulation of protein degradation is essential for controlling functional proteostasis (Labbadia & Morimoto, 2015). Proteins are degraded by two pathways: the ubiquitin-proteasome system (UPS) and the autophagy-lysosome pathway (ALP) (Dikic, 2017). In general, the UPS is primarily used to degrade short-lived, misfolded, or damaged proteins, whereas the ALP is used to remove larger components like protein aggregates or damaged organelles (Dikic, 2017). Proteins needing to be sent for degradation to the proteasome are tagged with a residue of the ubiquitin protein that the proteasome can then recognize and begin a series of enzymatic reactions to degrade the targeted protein (Wang & Le, 2019). The process of ubiquitination is comprised of three enzymes: the E1 enzyme that activates ubiquitin, the E2 molecule that binds to the ubiquitin, and the E3 ligase that transfers the ubiquitin from the E2 molecule to the targeted protein. There are hundreds of E3 ligases that bind to specific substrates for ubiquitin transfer (Wang & Le, 2019). On the other hand, ALP utilizes bi-layered membrane vesicles called autophagosomes that engulf damaged proteins or organelles. Autophagosomes can then directly fuse to the lysosome for degradation where the degraded contents can be recycled back into the cell. The regulatory mechanism and selectivity for autophagy is highly complicated and specific (Wang & Le, 2019). Overall, disposal of damaged proteins and organelles through both systems is necessary for proper proteostasis in the cell.

Protein maintenance and the heat shock response

One of the main functions of the proteostasis network is to prevent the formation of misfolded proteins or toxic aggregates that form from stress or disease. To do this, the cell has multiple stress response pathways to ensure proper protein maintenance, including the heat shock response (HSR) and the unfolded protein response (UPR). The UPR is a signal transduction pathway that senses and responds to abnormal protein misfolding or unfolding in the endoplasmic reticulum (ER) (Hetz, Zhang, & Kaufman, 2020). The UPR utilizes three main signaling pathways: via PERK to attenuate protein synthesis in cell (Kaufman, 2002); via IRE1α to reduce protein abundance in the ER (Hollien & Weissman, 2006); and via ATF6 to promote transcription of ER chaperones and enzymes to promote protein folding and degradation (J. Wu et al., 2007).

Similarly, the unfolded protein response in the cytosol, also known as the heat shock response (HSR), responds to proteotoxic stress in the cytosol. The HSR is a highly conserved response to stressors such as heat shock, heavy metals, and oxidative stress (Labbadia & Morimoto, 2015). Genes encoding for molecular chaperones are induced by heat shock transcription factor 1 (HSF1) and aid in the re-folding or degradation of damaged proteins. Upon stress, HSF1 trimerizes and induces transcription of molecular chaperones, including heat shock proteins (HSP) HSP70, HSP90, and HSP60 (Westerheide, Anckar, Stevens, Sistonen, & Morimoto, 2009). These heat shock proteins guide protein folding and degradation to equilibrate the proteostasis of the cytosol. Upon attenuation, HSF1 is degraded by the UPS (Kourtis, Moubarak, et al., 2015). The transcriptional activity of HSF1 is stress inducible and highly regulated (Westerheide, Raynes, Powell, Xue, & Uversky, 2012).

History of the Heat Shock Response

The HSR was initially discovered in the 1960s by Ferruccio Ritossa, who was studying DNA in *Drosophila melanogaster* (Ritossa, 1996). While studying fruit fly chromosomes, a colleague mistakenly increased the temperature of the incubator the fruit flies were kept in and Ritossa observed a novel puffing pattern in the chromosomes. The puffing of the chromosomes indicated that there was an increase in transcriptional activity with increased temperatures (Ritossa, 1996). Then in the 1970s, with the radiolabeling of mRNA and proteins, global changes in transcription and translation were observed to occur after heat shock (Lewis, Helmsing, & Ashburner, 1975; Spradling, Pardue, & Penman, 1977). This included the upregulation of certain genes and their protein products which were subsequently called heat shock proteins. The Morimoto laboratory found a particular HSP with a molecular weight of 70 kDa, HSP70, to be highly induced upon heat shock (Mosser, Theodorakis, & Morimoto, 1988). While examining the promoter region of *hsp70*, the group discovered a series of three inverted repeats of the sequence nGAAn, which they coined as heat shock elements (HSEs) (B. J. Wu, Kingston, & Morimoto, 1986). This ultimately led to the discovery of the transcription factor that binds to these regions, heat shock factor 1 (Goldenberg et al., 1988; Parker & Topol, 1984; Wiederrecht, Shuey, Kibbe, & Parker, 1987). From here, work on the HSR and HSF1 has grown to better understand its mechanism, regulation, and implications in many diseases.

HSF1 Structure and Domains

The structure of HSF1 is defined by its functional domains that allow for regulation of the protein-quality control machinery to regulate gene expression. The winged helix-turn-helix DNA binding domain (DBD) is at the amino-terminal end of HSF1 and allows for binding at HSEs along the DNA (Vuister et al., 1994). Because HSF1 trimerizes upon activation, a trimerization

domain is located adjacent to the DBD. This domain contains hydrophobic leucine-zipper-like heptad repeats (HR-A/B) that allow for oligomerization (Sorger & Nelson, 1989). In order to activate target gene expression, HSF1 also contains a transactivation domain (TAD) at the carboxyl-terminal that binds to auxiliary factors for activation (Sullivan, Weirich, Guyon, Sif, & Kingston, 2001). A regulatory domain (RD) is also present to negatively regulate the TAD (Shi, Kroeger, & Morimoto, 1995).

HSF1 Activation and Attenuation Cycle

HSF1 activation

HSF1 is found in both the nucleus and cytoplasm and rests in the inactive state, which is mostly as a monomer (Anckar & Sistonen, 2011). Monomeric HSF1 binds to a variety of chaperones including heat shock proteins, HSP70 and HSP90. Upon heat stress, HSF1 is activated by trimerizing and becoming DNA-binding-competent (Joutsen & Sistonen, 2019). Active HSF1 accumulates in the nucleus due to its nuclear localization sequence, and trimeric HSF1 can then bind to HSEs found in the promoter regions of its target genes (Amin, Ananthan, & Voellmy, 1988; Mercier, Winegarden, & Westwood, 1999). HSF1 activation is also highly dependent on post-translational modifications (PTMs) or other protein-protein interactions (Joutsen & Sistonen, 2019). It is still unclear the exact mechanism of HSF1 activation, but there are several proposed mechanisms that could be dependent on stress-type. It is suggested that HSF1 binding to HSPs keeps HSF1 in its inactive state. Upon heat stress, the HSPs get titrated away from HSF1 to bind to the increased accumulation of misfolded proteins in the cell. This allows for HSF1 to trimerize and activate (Bharadwaj, Ali, & Ovsenek, 1999; Sivery, Courtade, & Thommen, 2016; Zou, Guo, Guettouche, Smith, & Voellmy, 1998). Another proposed mechanism is that HSF1 is a thermosensor and activates by sensing changes in temperature

(Hentze, Le Breton, Wiesner, Kempf, & Mayer, 2016). Overall, HSF1 activation is highly regulated and allows for specific induction of the HSR in the cell.

HSF1 localization and nuclear stress bodies

Upon heat stress and as HSF1 activates, scientists have observed distinct HSF1 foci formation in the nucleus called nuclear stress bodies (nSBs) (Jolly, Usson, & Morimoto, 1999). nSBs are a hallmark of HSF1 activation (Biamonti & Vourc'h, 2010; Deonarine, Walker, & Westerheide, 2021; Jolly et al., 2004; Jolly et al., 1999; Morton & Lamitina, 2013). In mammalian cells, the resolution of nSBs correlates with HSF1 activity, transcription of *hsp* target genes, and cell survival at the single cell level (Gaglia et al., 2020). A recent mammalian study discovered the existence of both HSF1 nSBs at non-*hsp* gene loci and smaller HSF1 condensates at transcriptionally active *hsp* gene loci upon heat shock (H. Zhang et al., 2022). In this study, HSF1 in the smaller condensates was found to colocalize with transcription apparatus factors, including RNA Pol II, BRD4, MED1, and CYCT1 (H. Zhang et al., 2022). The precise function of nSBs and HSF1's localization to nSBs after activation has yet to be fully elucidated.

HSF1 attenuation

Once the HSR has been activated and the HSP target proteins have been translated to aid in the refolding of misfolded proteins, the HSR requires inactivation. Through the modification of multiple inhibitory PTMs and other proteins including HSPs, HSF1 gets inactivated, dissociates from the DNA, and gets targeted to the proteasome for degradation. With an increase in free HSPs in the cell, these HSPs can subsequently re-associate with HSF1 and inhibit its activation in a feedback loop (Sivery et al., 2016). Also, many PTMs aid in the removal of HSF1 from the DNA and prevent transcription from occurring (Raychaudhuri et al., 2014; Westerheide et al.,

2009). Degradation of HSF1 is also a pathway of HSF1 attenuation that has not fully been elucidated. Studies in neurodegenerative disease have examined the aberrant mechanisms of HSF1 degradation, but it is still unclear where HSF1 degradation occurs and the extent of which HSF1 is recycled during attenuation (Gomez-Pastor et al., 2017; E. Kim et al., 2016). Ultimately, inactive HSF1 remains in the cytosol and nucleus until needed for further activation.

Post-translational Modifications of HSF1

Like many transcription factors, HSF1 is highly regulated via post-translational modifications (PTMs). These modifications have been shown to contribute to every step in the activation of HSF1 from oligomerization to DNA binding to attenuation as well as its deactivation (Joutsen & Sistonen, 2019). Theses PTMs are added to all HSF1 domains for their regulation, and HSF1 is subjected to many PTMs including phosphorylation, acetylation, ubiquitination, and sumoylation, many with a complex set of roles in activation or attenuation of HSF1 (Joutsen & Sistonen, 2019).

Acetylation of HSF1 via Lysine Acetyltransferases

Acetylation refers to the reversible addition of an acetyl group to the side of a lysine residue of a protein that causes neutralization of the positive charge of lysine (Narita, Weinert, & Choudhary, 2019). This modification can have a variety of effects on the protein's stability, conformation, or function. Proteins and histones get acetylated by lysine acetyltransferases (KATs) and conversely removed by lysine deacetylases (Narita et al., 2019). Acetylation has been shown to have a variety of functions in regulating HSF1, with 11 lysine residues of HSF1 that have been shown to be acetylated (Raychaudhuri et al., 2014; Westerheide et al., 2009). Under non-stressed conditions, HSF1 levels are tightly controlled by the acetylation of specific lysine residues (K208

and K298) (Raychaudhuri et al., 2014). These acetylation sites mediate HSF1 stabilization by preventing its degradation by the proteasome. As well, these acetylation events were found to be acetylated by the histone acetyltransferase EP300 (Raychaudhuri et al., 2014). This histone acetyltransferase was also found to acetylate K80 of HSF1 which prevents HSF1 binding to the DNA, aiding in the attenuation of the HSR (Westerheide et al., 2009).

The effects of acetylation at K80 and K118 can be reversed by the deacetylase, sirtuin (SIRT1), which has been shown to deacetylate HSF1 at these sites (Westerheide et al., 2009). SIRT1 was found to prolong the HSR by preventing HSF1 attenuation. When SIRT1 levels are depleted, the ability of HSF1 to bind to target gene promoter regions is greatly reduced (Westerheide et al., 2009). Similarly, the age-related decline in HSF1 levels is thought to partially be affected by a decrease in SIRT1 levels with age, leading to an increase in K80 acetylation-dependent proteasomal degradation in neuronal cells (Zelin & Freeman, 2015).

Phosphorylation of HSF1 via Protein Kinases

Phosphorylation of proteins occurs by protein kinases that catalyze the transfer of an additional phosphate group to their substrates (Cheng, Qi, Paudel, & Zhu, 2011). There are approximately 23 known sites of phosphorylation of HSF1, most of which are found in the regulatory domain (Guettouche, Boellmann, Lane, & Voellmy, 2005). Upon heat shock, hyperphosphorylation of HSF1 occurs with HSF1 activation and DNA binding (Cotto, Kline, & Morimoto, 1996). However, HSF1 can still be transcriptionally active even in the absence of any phosphorylation event. It is thought that HSF1 phosphorylation is more of a fine-tuning mechanism for its activity (Budzynski, Puustinen, Joutsen, & Sistonen, 2015). There are a variety of protein kinases that have been found to directly interact with HSF1 and can phosphorylate HSF1 at similar residues but in distinct contexts. The serine residues S303 and S307 can be phosphorylated by many

protein kinases, including GSK3β, casein kinase 2 (CK2), MEK1 and ERK1 (Chu, Zhong, Soncin, Stevenson, & Calderwood, 1998; Gomez-Pastor et al., 2017). These phosphorylation events lead to the ubiquitination of HSF1 and to its degradation via the proteasome. In Huntington's disease, phosphorylated HSF1 at these serine residues is a substrate for FBXW7, a component of the E3 ubiquitin ligase system (Gomez-Pastor et al., 2017).

Sumoylation of HSF1

Sumoylation is another type of PTM that involves the addition of a small ubiquitin-like modifier to specific lysine residues (Yang et al., 2017). HSF1 is primarily sumoylated on K298 but can also be sumoylated on the K126 residue (Hong et al., 2001). K298 sumolyation is a part of the phosphorylation-dependent sumoylation motif (PDSM), where the phosphorylation of S303 is required for SUMO-1 to be added at K298. Sumoylation at this site is not required for HSF1 activity but functions as a negative regulator of its transactivation activity (Hong et al., 2001). Additional sites of HSF1 sumoylation have recently been identified by a screen, but their functions have not been examined (Hendriks & Dingemans, 2017).

Ubiquitination of HSF1

The abundance and activity of HSF1 is also partially regulated by the ubiquitin-proteasome system to degrade HSF1 in the cell (Raychaudhuri et al., 2014). Ubiquitination of HSF1 on its lysine residues lead to its degradation by the proteasome. Two ubiquitin ligases, FBXW7 and NEDD4, have been shown to interact and ubiquitinate HSF1 (Gomez-Pastor et al., 2017; E. Kim et al., 2016). The sites of HSF1 ubiquitination are unknown, but the interaction between FBXW7 and HSF1 is dependent on the phosphorylation of S303 and S307 as mentioned previously (Gomez-Pastor et al., 2017). It was found that HSF1 degradation is an important step in its

attenuation, where previously HSF1 was just thought to revert back to its monomeric state (Kourtis, Strikoudis, & Aifantis, 2015).

HSR Regulation in Aging and Disease

In neurodegenerative disease

Defects in proteostasis and the HSR that occur with aging are central to many human diseases, including Alzheimer's disease, Huntington's disease, and Parkinson's disease (Neef, Jaeger, & Thiele, 2011). These neurodegenerative diseases (NDDs) are proteotoxic diseases hallmarked by increased protein misfolding and aggregation (Muchowski & Wacker, 2005). Huntington's disease is hallmarked by the abnormal polyglutamine expansion in the Huntingtin protein in the N-terminal domain. These polyglutamine expansions can aggregate together causing large inclusion bodies of aggregating Huntingtin protein (Havel, Li, & Li, 2009). Alzheimer's disease results from the aggregation of the toxic protein amyloid-beta. The accumulation and aggregation of this protein causes neuronal loss in the brain leading to dementia or loss of cognition (Mavroudis et al., 2010). Parkinson's disease is hallmarked by the aggregation of the protein alpha-synuclein that form Lewy bodies and leads to loss of dopaminergic neurons in the brain (E. Kim et al., 2016).

This protein toxicity of these neurodegenerative diseases leads to neuronal dysfunction and subsequent neuronal death, causing various symptoms for patients from dementia to tremors. Protein toxicity disrupts the proteostasis in the cell that is needed for its proper function (Labbadia & Morimoto, 2015). Current drug treatments of these neurodegenerative diseases combat the symptoms associated with these diseases but not the underlying proteotoxicity causing these symptoms (Gomez-Pastor, Burchfiel, & Thiele, 2018). Therefore, novel

therapeutic drugs are currently needed to treat these diseases and the underlying proteostasis dysfunction caused by the proteotoxicity of the protein aggregates. Studies in the heat shock response have demonstrated therapeutic potential in enhancing the protein folding capacity of cells (Neef et al., 2011).

It has been widely documented that HSF-1 and heat shock protein activity is impaired in aging and neurodegenerative diseases (Anckar & Sistonen, 2011). Downregulation of the heat shock response in these protein misfolding diseases contributes to the protein aggregation and overall neuronal dysfunction and death (Gomez-Pastor et al., 2017). Many studies have found that upregulating HSF1 or HSP activity has beneficial effects on the proteotoxicity of the diseases (Neef et al., 2011). Previous studies have shown that HSF1 levels and HSP levels are depleted in Alzheimer's, Huntington's, and Parkinson's disease patient brains (Gomez-Pastor et al., 2017; Jiang et al., 2013; E. Kim et al., 2016). In Huntington's and Parkinson's disease, the depletion of HSF1 is due to its degradation, but it is unclear if the same is true in Alzheimer's disease. Abnormal degradation of HSF1 in Huntington's was found to be mediated by proteasomal degradation via the E3 ligase FBXW7 (Gomez-Pastor et al., 2017). Similarly, HSF1 phosphorylation at S303 and S307 was found to mediate this degradation by FBXW7. HSF1 phosphorylation was found to be modified by casein kinase 2. Both CK2 and FBXW7 are upregulated in Huntington's disease (Gomez-Pastor et al., 2017).

HSF1 degradation in Parkinson's disease was found to involve the E3 ligase NEDD4, which is upregulated in the diseased patients (E. Kim et al., 2016). It is unclear if this HSF1 degradation also requires HSF1 phosphorylation, although it has been reported that CK2 expression is increased in Parkinson's disease as well (Lee et al., 2004). For Alzheimer's disease, it is unknown if HSF1 is degraded or if HSF1 phosphorylation mediates its degradation, but similar

to the other disease models, HSF1 protein levels are decreased and CK2 levels are increased in Alzheimer's patients (Jiang et al., 2013; Rosenberger et al., 2016). It is also unclear if there are other E3 ligases that also aid in the degradation in these diseases. Understanding how HSF1 is being regulated in neurodegenerative disease could provide insight into novel therapeutics to reduce or prevent the protein aggregation associated with neurodegenerative disease.

In cancer

In contrast to decreased levels of HSF1 found in neurodegenerative disease, HSF1 levels are increased in many cancers (Mendillo et al., 2012; Meng, Gabai, & Sherman, 2010). Similarly, increased chaperone expression has been observed in a variety of different cancers, aiding in the increase of protein synthesis that occurs in these cancers (Whitesell & Lindquist, 2005). Malignant cells are prone to proteotoxic damage and stress and in general require a higher amount of HSPs to function in their unstable environment (Whitesell & Lindquist, 2005). HSF1 and its target proteins have been well studied in cancer. Overall, a decrease of HSF1 protects against tumorigenesis and malignancy (Dai, Dai, & Cao, 2012). Thus, identifying specific HSF1 therapeutic targets has large appeal.

C. elegans as a Model Organism

Experimental advantages of C. elegans

C. elegans is a powerful model organism to study cellular processes like the heat shock response. Their short life cycle (3-4 days) and lifespan (2-3 weeks) allows for rapid aging studies. Their transparent anatomy allows for *in vivo* visualization of fluorescently tagged proteins via fluorescence microscopy (Nussbaum-Krammer & Morimoto, 2014). Similarly, the different tissue types can be easily distinguished throughout the worm anatomy allowing for tissue-

specific experimentation. *C. elegans* was the first multicellular organism to have its genome sequenced. The full sequenced genome and mutant worm strains are freely available in public databases and resources. Approximately 80% of the proteins encoded in the *C. elegans* genome are conserved in vertebrates as well. Gene expression can be targeted through RNA interference (RNAi) by either feeding worms bacteria that produce double stranded RNA (dsRNA) or by injection of dsRNA into the worm (Kamath et al., 2003).

Neurodegenerative disease models in C. elegans

Many age-related protein misfolding disorders and neurodegenerative diseases are modeled in the worm, and a large number of these strains have fluorescently tagged protein aggregation that allows for visualization (J. Li & Le, 2013). The fluorescently tagged proteins that are linked to these diseases are generally aggregating proteins that can be easily visualized in the cells. Many of these aggregating proteins cause toxicity that results in paralysis or tissue damage that can be measured (Brignull, Morley, & Morimoto, 2007). For example, there are a wide variety of *C. elegans* neurodegenerative disease models that allow for whole organism assessment of the disease state. Many of these worm disease models mimic the production of the disease protein aggregates throughout the worm's life cycle (2-3 weeks) through transgenic expression (J. Li & Le, 2013). This allows for the protein aggregates to be expressed in certain tissue types like the muscle or neuron cells. The tissue-specificity of these models can be beneficial when examining whole-organism effects.

Regulation of the HSR by HSF-1 in C. elegans

The heat shock response in highly conserved in *C. elegans.* Studies in *C. elegans* have shown that HSF-1 is an essential protein that plays a major role in development and organismal

physiology. HSF-1 is required for heat shock response activation and plays an important role in development and aging (Hsu, Murphy, & Kenyon, 2003). Knockdown of HSF-1 results in a stress-sensitive and rapid aging phenotype (Garigan et al., 2002). Overexpression of HSF-1 increases longevity and cytoprotection of the worm (Morley & Morimoto, 2004). Structurally, HSF-1 is very similar to its mammalian homolog. Both contain a DNA-binding domain, an oligomerization domain, and a transactivation domain (Hajdu-Cronin, Chen, & Sternberg, 2004). HSF-1 in *C. elegans* has been shown to also require trimerization and hyperphosphorylation for activation after heat shock (Morton & Lamitina, 2013). There have been studies identifying regulators of the heat shock response (Guisbert, Czyz, Richter, McMullen, & Morimoto, 2013); however, there is still much to understand about how *C. elegans* HSF-1 is regulated and activated. How these regulators of the heat shock response affect the physiology of the worm at the organismal level has yet to be elucidated.

CBP-1 Regulation in C. elegans

The activity of CREB binding protein CBP-1, the *C. elegans* homolog of CBP/p300, is highly conserved and makes *C. elegans* a useful model organism to study the regulation of CBP-1 during stress and aging. HSF-1 has been shown to interact with CBP-1 in lifespan regulation (M. Zhang et al., 2009); however, the mechanism by which CBP-1 regulates HSF-1 has not been examined. CBP-1 in *C. elegans* functions as a chromatin remodeler and lysine acetyltransferase that can regulate transcription (Victor et al., 2002). CBP-1 is an essential protein for embryonic development, cell differentiation, and aging, and knockdown of cbp-1 significantly reduces lifespan (Cai et al., 2019; Shi & Mello, 1998; Victor et al., 2002; M. Zhang et al., 2009). CBP-1 also acts in multiple stress response pathways, including the mitochondrial unfolded protein response and the oxidative stress response (Ganner et al., 2019; T. Y. Li et al., 2021). Although

CBP-1 interactions with HSF-1 have been described, its role, as well as the potential role of other lysine acetyltransferases, in regulating HSF-1 and the HSR are still unknown.

CHAPTER TWO: THE P300/CBP LYSINE ACETYLTRANSFERASE CBP-1 REGULATES THE HEAT SHOCK RESPONSE IN *C. ELEGANS*

Text adapted from manuscript submitted to Frontiers in Aging, section Aging, Metabolism and Redox Biology.

Abstract

The decline of proteostasis is a hallmark of aging that is, in part, affected by the dysregulation of the heat shock response (HSR), a highly conserved cellular response to proteotoxic stress in the cell. The heat shock transcription factor HSF-1 is well-studied as a key regulator of proteostasis, but mechanisms that could be used to modulate HSF-1 function to enhance proteostasis during aging are largely unknown. In this study, we examined lysine acetyltransferase regulation of the HSR and HSF-1 in *C. elegans*. We performed an RNA interference screen of lysine acetyltransferases and examined mRNA expression of the heat-shock inducible gene *hsp-16.2*, a widely used marker for HSR activation. From this screen, we identified one acetyltransferase, CBP-1, the *C. elegans* homolog of mammalian CREB-binding protein CBP/p300, as a negative regulator of the HSR. We found that while knockdown of CBP-1 decreases the overall lifespan

of the worm, it also enhances heat shock protein production upon heat shock and increases thermotolerance of the worm in an HSF-1 dependent manner. Similarly, we examined a hallmark of HSF-1 activation, the formation of nuclear stress bodies (nSBs). In analyzing the recovery rate of nSBs, we found that knockdown of CBP-1 enhanced the recovery and resolution of nSBs after stress. Collectively, our studies demonstrate a role of CBP-1 as a negative regulator of HSF-1 activity and its physiological effects at the organismal level upon stress.

Introduction

One of the hallmarks of aging is the dysregulation of protein homeostasis, or proteostasis, in the cell which is critical for cell survival and function (Lopez-Otin, Blasco, Partridge, Serrano, & Kroemer, 2013). The heat shock response (HSR) is a key player in the proteostasis network, known to play a role in a variety of physiological processes, including development, reproduction, aging, and age-related diseases (Joutsen & Sistonen, 2019). The HSR is a highly conserved cellular response that maintains proteostasis in the cell through the activation of heat shock transcription factor 1 (HSF1). HSF1 is the master regulator of the HSR and when activated, drives the expression of heat shock proteins (HSPs) that act as molecular chaperones to restore proteostasis after stress (Hartl, Bracher, & Hayer-Hartl, 2011). HSF1 has been implicated in a wide array of age-related diseases, including neurodegenerative diseases, metabolic diseases, and cancer (Gomez-Pastor et al., 2018). Understanding HSF1 regulation with aging may be useful when developing therapeutic strategies for such diseases.

The transcriptional activity of HSF1 is stress-inducible and highly regulated (Westerheide et al., 2012). Human HSF1 is regulated in part through post-translational modifications. These modifications include acetylation, phosphorylation, and sumoylation, and they function in both the activation and attenuation of HSF1 (Gomez-Pastor et al., 2018). Studies have shown multiple

site-specific, reversible acetylation modifications on HSF1 that affect its overall protein stability and attenuation (Raychaudhuri et al., 2014; Westerheide et al., 2009; Zelin & Freeman, 2015). Under non-stress conditions, HSF1 levels are stabilized by the acetylation of Lys208 and Lys298 by the lysine acetyltransferase (KAT) CBP/p300 (Raychaudhuri et al., 2014). During stress, CBP/p300 also mediates the acetylation of Lys80 of HSF1, which aids in inhibiting HSF1 binding to DNA to attenuate the HSR (Raychaudhuri et al., 2014; Westerheide et al., 2009). There are also multiple other known sites of HSF1 acetylation where the effect of acetylation has yet to be elucidated.

The activity of HSF-1, the C. elegans homolog of HSF1, is highly conserved and makes *C. elegans* a useful model organism to study the regulation of HSF-1 during stress and aging. HSF-1 has been shown to interact with CREB binding protein CBP-1, the *C. elegans* homolog of CBP/p300, in lifespan regulation (M. Zhang et al., 2009); however, the mechanism by which CBP-1 regulates HSF-1 has not been examined.

CBP-1 in *C. elegans* functions as a chromatin remodeler and lysine acetyltransferase that can regulate transcription (Victor et al., 2002). CBP-1 is an essential protein for embryonic development, cell differentiation, and aging, and knockdown of cbp-1 significantly reduces lifespan (Cai et al., 2019; Shi & Mello, 1998; Victor et al., 2002; M. Zhang et al., 2009). CBP-1 also acts in multiple stress response pathways, including the mitochondrial unfolded protein response and the oxidative stress response (Ganner et al., 2019; T. Y. Li et al., 2021). Although CBP-1 interactions with HSF-1 have been described, its role, as well as the potential role of other lysine acetyltransferases, in regulating HSF-1 and the HSR are still unknown.

In this study, we utilized *C. elegans* to screen for lysine acetyltransferase modulators of the HSR. We identified a role of CBP-1 in negatively regulating the HSR in *C. elegans*, confirming the

importance of this regulator in this stress response pathway. Collectively, our studies demonstrate the ability of CBP-1 to regulate the HSR in an HSF-1 dependent-manner and highlight its effects on stress resistance and longevity.

Methods

C. elegans strains and maintenance

The following strains were used in this study: N2 (Bristol), PS3551 - *hsf-1*(sy441), MH2430 – *cbp-1* (ku258), SDW015 - *hsf-1*(asd002(*hsf-1::GFP* + *unc-119*(+)), and SDW173. The MH2430 strain was outcrossed three times to the N2 wildtype strain to generate the SDW173 strain. Strains were maintained at 20°C on standard NGM plates seeded with *Escherichia coli* OP50-1. The synchronous population of nematodes was obtained by bleach synchronization and plated for 19 hrs on NGM plates without food.

RNA interference (RNAi)

Synchronous L1 nematodes were grown on standard NGM plates seeded with OP50-1 bacteria for 19 hrs to prevent potential RNAi-mediated effects on early development. Worms were transferred onto standard NGM plates supplemented with 25 µg/ml carbenicillin and 1 mM isopropyl-beta-ᴅ-thiogalactopyranoside (IPTG) and seeded with either HT115 bacteria containing an empty vector (EV/L4440 control) or with sequence-verified gene-specific RNAi strains isolated from the Ahringer RNAi library (J. Ahringer, University of Cambridge, Cambridge, U.K.), as previously described (Kamath et al., 2003). To induce dsRNA production, HT115 bacteria were supplemented with 1 mM IPTG shaking at 37°C for 1 hour before seeding.

RNA isolation and quantitative PCR

RNA was extracted with TRIzol® reagent (Ambion®, cat# 15,596–026) by standard protocol. RNA was reverse-transcribed using a High Capacity cDNA Reverse Transcription Kit (Applied Biosystems, cat# 4,368,814). cDNA was diluted to 100 ng/µl to be used as a template for qRT–PCR performed with the StepOne Plus Real-time PCR system (Applied Biosystems, cat # 4,376,600) using iTaq™ Universal SYBR® Green Supermix (Bio-Rad, cat# 1,725,121) according to the manufacturer's instructions. Expression levels were analyzed via qPCR using the ΔΔCt method. The housekeeping gene *cdc-42* (R07G3.1) was used for normalization. Results show averages of independent biological triplicates performed in technical triplicates. Statistical analysis was performed with GraphPad (GraphPad Software, https://www.graphpad.com) using an unpaired Student's t-test.

Primers used: *hsp16.2* (Y46H3A.3) Fwd: ACGCCAATTTGCTCCAGTCT, Rvs: TGATGGCAAACTTTTGATCATTGT; *hsp-70* (C12C8.1) Fwd: TTCAATGGGAAGGACCTCAACT, Rvs: GGCTGCACCAAAGGCTACTG; *cdc-42* (R07G3.1) Fwd: CTTCTGAGTATGTGCCGACAGTCT, Rvs: GGCTCGCCACCGATCAT; *hsp16.48* (T27E4.3) Fwd: TTGGAGAAATGCTGATCACAACTC, Rvs: TTTTTAGTTCTCTTCCATCCAATTCA; F44E5.5 Fwd: CTTCATGCAAAGCTATTGGTATCG, Rvs: CTTCCGAGTTGGCGAGGAT; *cbp-1* (R10E11.1) Fwd: GCAGCGAAAACGGAGGAA, Rvs: GCATGGAACAAATGTGGAGTCTT; *hsf-1* (Y53C10A.12) Fwd: TGCAGCCAGGATTGTCGA, Rvs: GGCGGCGCAAAAGTCTATT; *hat-1* (M03C11.4) Fwd: ACGGACTTGCTGTCGTTAAA, Rvs: CCGAAGATTGTCTCCTCATCTC; *kat-1* (T02G5.8) Fwd: CCACATCTGCTGCACTATCA, Rvs: GCAGTTACCGAAGAGAGAGAAG; *taf-1* (W04A8.7)

Fwd: TACGAGGCCACAGCTTATTG, Rvs: CGCTTCTCCTCCTTATACTGTTC; *mys-1* (VC5.4) Fwd: CGAGCTGCAAATGGTTCAATTA, Rvs: GTAGCTCACACGACGCTAAA; *mys-2* (K03D10.3) Fwd: GGAGCGAAAGAGCTCATGTATT; Rvs: GCTCGACTACCACTTCGTTTAC; *mec-17* (F57H12.7) Fwd: GGTCATCAGAGCAAGGGAAA, Rvs: TTGGCCTGATGAGCTCTATTG; *atat-2* (W06B11.1) Fwd: GTTCAGCTGTGTCCAGTCAT, Rvs: TAACATATCCTGGCGCATCAA; T02G5.4 Fwd: GCAGTTACCGAAGAGAGAGAAG, Rvs: CCACATCTGCTGCACTATCA; *hsp-1* (F26D10.3) Fwd: TCAAGAGAAACACCACCATCC, Rvs: GGCACGTTCTCCTTCGTAAA; *hsp-90* (C47E8.5) Fwd: AGTACTGCGTCCAACAACTC, Rvs: TCTTCTCCTCCTCGGTTTCT

Thermotolerance analysis

Thermotolerance was tested by exposing Day 1 animals to 37°C heat shock for 3.5 hours and then determining survival 48 hours later by assessing response to a gentle touch. For each trial, ~100 randomly selected individual animals were assessed for the fraction alive (live/total). Thermotolerance assay data reflects three biologically independent trials. Data was plotted as the % survival using GraphPad Prism (GraphPad Software, https://www.graphpad.com) and was analyzed with a two-tailed *t* test.

Lifespan analysis

All lifespan assays were performed at 20°C with approximately 100 worms per condition in biological triplicate. Animals were transferred to fresh plates daily for 5 days to avoid progeny contamination. Adult worms were scored approximately every day and counted as dead when no response was observed by poking with a platinum wire. The average survivability of three

replicates was plotted using OASIS 2 (https://sbi.postech.ac.kr/oasis2/) (Han et al., 2016), and statistical analysis was done by Log-rank (Mantel-Cox) Test.

Fluorescent microscopy and nuclear stress body assessment

Fluorescent images were obtained using a Keyence BZ-X fluorescent microscope. Animals were picked free of bacteria and anesthetized with 10 mM levamisole. Nuclear stress body formation was quantified by assessing for the presence of nuclear foci containing HSF-1::GFP in hypodermal cells. The heat shock conditions for nuclear stress body assessment were 15 min in a 33°C water bath on plates wrapped in parafilm. After anesthetizing and placing the cover slip on top of the worms, they were imaged within 10–15 min to avoid the formation of nuclear stress bodies which may be due to hypoxia or other cytotoxic stress (n=~10 worms per condition). Quantification was performed in GraphPad Prism (GraphPad Software, www.graphpad.com) and **s**ignificance was determined using 2-way ANOVA.

Thrashing assay

Thrashing/motility was tested by placing 15 Day 1 animals onto a drop of nematode growth media (NGM) buffer on a glass slide and measuring the number of body bends/30 seconds after a 1-minute recovery period. Thrashing data reflects three biologically independent trials. Data was plotted as boxplots using GraphPad Prism (GraphPad Software, https://www.graphpad.com) and was analyzed with a two-tailed *t* test.

Statistical analyses

Statistical analyses were carried out with GraphPad Software (GraphPad Software, La Jolla, CA, USA, https://www.graphpad.com) unless otherwise stated. All error bars are representative of standard deviation between independent biological replicates, as indicated.

Results

Targeted RNAi screen for lysine acetyltransferase modulators of the HSR identifies CBP-1

To identify lysine acetyltransferases that may regulate the HSR, we performed an RNA interference (RNAi) screen by targeting ~75% of all putative lysine acetyltransferases (KATs) in *C. elegans* using RNAi knockdown (Figure 2.1A). *C. elegans* KATs were identified by searching the *C. elegans* protein database for proteins containing conserved acetyltransferase domains to those of known human KATs (Sheikh & Akhtar, 2019). We utilized quantitative RT-PCR to assess the heat shock inducibility of *hsp-16.2* mRNA expression, a widely used marker of HSR activity, after KAT RNAi knockdown (Golden, Plagens, Kim Guisbert, & Guisbert, 2020). We induced RNAi 19 hours after the L1 stage until Day 1 of adulthood, when we extracted RNA before and immediately after a 1-hour heat shock at 33ºC to assess *hsp-16.2* expression (Figure 2.1B). Our KAT and *hsf-1* RNAi conditions suppress expression of their corresponding genes by about 50% (Figure A1, Figure A2). From this screen, we found no significant changes in *hsp-16.2* expression in non-heat shock conditions after KAT RNAi knockdown (Figure 2.1C). After heat shock, only RNAi for *cbp-1* (R10E11.1), the homolog of human CBP/p300 CREB binding protein, significantly altered the mRNA expression of *hsp16.2* expression, resulting in an increase in expression of approximately 2-fold (Figure 2.1C).

CBP-1 regulates the expression of multiple HSF-1 target genes in an HSF-1-dependent manner

To further examine the role of CBP-1 on the HSR, we examined how knockdown of *cbp*-1 affects various heat shock inducible HSF-1 target genes using qRT-PCR. The target genes tested, including *hsp-16.2*, *hsp.16.48, hsp-70,* and *F44E5.5* (an inducible *hsp-70* family gene), are highly inducible upon heat shock. We found that while *cbp*-1 RNAi didn't significantly change

the expression of the *hsp* target genes tested under basal conditions (Figure A3A), *cbp-1* RNAi did significantly increase the expression of these genes after heat shock as compared to EV control (Figure 2.2A). We also found that *cbp-1* knockdown does not affect *hsf-1* expression, or vice versa (Figure A1). HSF-1 also regulates the expression of a distinct subset of developmental genes independent of the HSR, including *hsp-1* and *hsp-90* (Li *et al* 2016). We found that *cbp-1* knockdown does not affect expression of these HSF-1 target genes (Figure A3B). Thus, CBP-1 is negatively regulating HSP but not HSF-1 expression after heat stress.

To determine whether this negative regulation of CBP-1 is mediated directly through HSF-1, we used the PS3551 worm strain containing a non-functional HSF-1 (J. B. Zhou et al., 2018). This mutant contains a point mutation in the HR-C domain of HSF-1 that causes the expression of a truncated non-functional HSF-1 mutant. We then measured the expression of *hsp-16.2* and *hsp-70* (C12C8.1) in response to *cbp-1* RNAi (beginning 19 hrs after L1) before and after heat shock in this mutant to determine dependence on HSF-1. While we found that knockdown of *cbp-1* increased *hsp-16.2* expression after heat shock with wildtype HSF-1 (Figure 2.1A), that increase is abolished with a nonfunctional HSF-1. Knockdown of *cbp-1* does not significantly increase *hsp-16.2* or *hsp*-70 (*C12C8.*1) expression after heat shock compared to control (Figure 2.2B). We conclude that CBP-1 depends on HSF-1 in order to regulate *hsp* gene expression.

Effect of CBP-1 and HSF-1 RNAi on thermotolerance and lifespan

We next wanted to test whether CBP-1 also regulates other physiological readouts of the HSR. To test for resistance to heat stress, we examined thermotolerance, physiological effect known to be modulated by HSF-1. To test this, we fed the worms *cbp-1*, *hsf-1*, or control RNAi from 19 hrs after L1 until Day 1 of adulthood prior to subjecting the worms to a lethal heat shock of 37ºC for 3.5 hours. After a 48-hour recovery, the worms were scored alive/dead after a gentle touch.

Compared to empty vector control RNAi-treated worms, *hsf-1* RNAi-treated worms had significantly reduced survival after heat shock (~20% decrease), as expected (Figure 2.3A). However, knockdown of *cbp-1* increased the % survival of the worms by ~40% (Figure 2.3A). Thus, knockdown of *cbp-1* increases thermotolerance.

We then performed a complimentary experiment, assessing how an increase in CBP-1 activity would affect thermotolerance. We utilized the MH3420 strain that contains two point mutations in *cbp-1,* resulting in a gain-of-function allele with increased KAT activity (Eastburn & Han, 2005). This strain was outcrossed three times with our laboratory N2 strain to create the SDW173 strain. N2 and SDW173 worms were synchronized and grown to Day 1 of adulthood then subjected to a lethal heat shock of 37ºC for 3.5 hours. We found that SDW173 worms had an ~20% decrease in percent survival as compared to N2 wildtype worms (Figure 2.3B). This suggests that an increase in CBP-1 acetyltransferase activity decreases thermotolerance. In summary, *cbp-1* RNAi activates thermotolerance, while a *cbp-1* gain-of-function mutant inhibits thermotolerance.

Previous studies have found that *cbp-1* RNAi reduces the lifespan of the worm (Cai et al., 2019; M. Zhang et al., 2009). We wanted to test whether this effect depends on HSF-1. Worms were fed with EV control, *cbp-1, hsf-1,* or *cbp-1/hsf-1* double RNAi from 19 hours after L1 throughout their lifespans. The worms were scored approximately every day starting at day 1 of adulthood for survival, and dead worms were scored when non-responsive to poking with a platinum wire. We found that *cbp-1* RNAi decreased lifespan to a significantly lesser extent than *hsf-1* RNAi (Figure 2.3C). However, the *cbp-1/hsf-1* double RNAi did not further reduce lifespan (Figure 2.3C).

cbp-1 RNAi increases recovery rate of nuclear stress bodies (nSBs) after heat shock

Upon activation of the HSR, HSF-1 undergoes localization changes and forms nuclear stress bodies (nSBs), a hallmark of HSF-1 activation (Deonarine et al., 2021). nSBs require HSF-1 binding and are a sign of activation of the HSR (Morton & Lamitina, 2013). After HSR activation, nSBs form within 5 minutes of stress detection and gradually dissolve until HSF-1 is diffuse in the nucleus (Figure 2.4A) (Deonarine et al., 2021). We examined the effect of *cbp-1* RNAi on the rate of nSB recovery after stress. We used the SDW015 (HSF-1::GFP) strain to visualize nSB formation before and after a 15-minute heat shock at 33ºC on Day 2 of adulthood. We utilized fluorescence microscopy to image hypodermal cells of the worm in 30-minute increments until the majority of cells containing nSBs had diffuse HSF-1::GFP expression in the nuclei (Figure 2.4A). After heat shock, control worms took an average of 1.7 hours to recover and resolve their nSBs, whereas worms fed *cbp-1* RNAi took an average of 1.1 hours to resolve nSBs (Figure 2.4B). Thus, knockdown of *cbp-1* significantly increased the rate of recovery of nSBs after heat shock.

cbp-1 RNAi does not alter motility or expression kinetics of hsp-16.2 or hsp-70 after heat shock

Since CBP-1 increases the rate of recovery of nSBs, we wanted to test whether CBP-1 also affected HSP expression kinetics after heat shock. We isolated RNA from Day 1 worms that were fed either control or *cbp-1* RNAi from 19hrs after the L1 stage. RNA was extracted from worms before and immediately after a 15-minute heat shock at 33°C. RNA was also collected in 30-minute increments after heat shock until 2 hours of recovery. We examined how *cbp*-1 knockdown affects the expression of *hsp-16.*2 and *hsp*-70 expression using RT-qPCR. We found that compared to EV control, knockdown of *cbp-1* did not significantly affect *hsp-16.2* or *hsp-70* mRNA expression after heat shock (Figure 2.5).

We also wanted to test whether CBP-1 affecting the worms motility. To test this, we fed the worms *cbp-1, hsf-1,* or control RNAi from 19 hrs after L1 until Day 1 of adulthood**.** We then placed the worms in a drop of NGM buffer and allowed them to recover for one minute before counting the number of body bends in 30 seconds. We found that there was no significant difference in motility between control, *cbp-1* RNAi, and *hsf-1* RNAi animals (Figure 2.6).

Discussion

Given the importance of post-translational modifications on HSF-1 regulation and function, we sought to elucidate the effect of lysine acetyltransferase regulation on the HSR. Here, we conducted a targeted RNAi screen for lysine acetyltransferase regulation of *hsp-16.2* expression levels and identified CBP-1 as a regulator of *hsp* expression. In addition, *cbp-1* knockdown also increased the expression of multiple other heat shock genes, increased thermotolerance, and improved the recovery rate of nuclear stress bodies after heat stress. Overall, these studies suggest a role for CBP-1 in negatively regulating HSF-1 activity during stress.

CBP-1 is widely known to be a transcriptional coactivator that aids in transcription (Victor et al., 2002). We further examined various other heat-shock inducible *hsp* expression and found that *cbp-1* knockdown increases the expression of multiple *hsp*s (*hsp-16.2, hsp.16.48, hsp-70,* and F44E5.5) after heat shock. This type of negative transcriptional regulation is a novel role for CBP-1 in *C. elegans*. However, human CBP/p300 has some characterized instances in which it negatively regulates transcription through effects on transcription factors. For example, acetylation of the elongation factor AFF1 by CBP/p300 inhibits transcription during genotoxic stress (Kumari, Hassan, Lu, Roeder, & Biswas, 2019).

CBP-1 is an essential protein that regulates multiple physiological processes including cell differentiation, embryonic development, metabolism, lifespan, and aging (Cai et al., 2019; Shi & Mello, 1998; Vora et al., 2013; M. Zhang et al., 2009). Specifically, CBP-1 interacts with DAF-16 and HSF-1 to regulate lifespan during caloric restriction (M. Zhang et al., 2009). Similarly, our results suggest that CBP-1 and HSF-1 work in the same pathway to regulate lifespan. While our work suggests that CBP-1 negatively regulates the HSR, our lifespan results suggest that it positively affects lifespan and aging. This was unexpected, as activating the HSR generally protects from aging (Hsu et al., 2003; Morley & Morimoto, 2004). Since CBP-1 plays a positive role in a variety of physiological pathways that control aging (Cai et al., 2019; Ganner et al., 2019; T. Y. Li et al., 2021; M. Zhang et al., 2009; L. Zhou, He, Deng, Pang, & Tang, 2019), it may be that the effects on these pathways are overriding the effects of CBP on HSF-1 and HSP expression in terms of life span regulation. It will be informative in future work to determine how the regulation of HSF-1 activity by CBP-1 can benefit aging and potentially lifespan in the worm.

While our data indicates that CBP-1 regulates HSF-1 activity, the mechanism of this regulation is still unknown. CBP-1 could directly acetylate HSF-1 as one potential mechanism. Mammalian CBP/p300 acetylates HSF-1 under both stress and non-stress conditions to both stabilize HSF-1 and attenuate HSF-1 from the DNA (Raychaudhuri et al., 2014; Westerheide et al., 2009). CBP/p300 acetylation of HSF1 could be conserved in *C. elegans* and function to attenuate HSF-1 activity. While human CBP/p300 also acts as a scaffolding protein to recruit the transcriptional machinery (Holmqvist & Mannervik, 2013), it is likely that worm CBP-1 regulation of the HSR requires CBP-1 acetyltransferase activity since we found that the SDW173 mutant containing CBP-1 with hyperactive KAT activity decreased thermotolerance. There is also the possibility of

CBP-1 regulating HSF-1 through an indirect regulator, as CBP-1 also binds to a multitude of other factors including the stress-responsive factors SKN-1 and DAF-16 (Ganner et al., 2019; Nasrin et al., 2000). Future work to uncover the mechanism behind HSF-1 regulation will allow for a more detailed analysis of the role of CBP-1 during stress and aging.

A hallmark of HSF1 activation in both mammalian cells and *C. elegans* is the formation and resolution of nuclear stress bodies (nSBs) containing HSF1 (Biamonti & Vourc'h, 2010; Deonarine et al., 2021; Jolly et al., 2004; Jolly et al., 1999; Morton & Lamitina, 2013). In mammalian cells, the resolution of nSBs correlates with HSF1 activity, transcription of *hsp* target genes, and cell survival at the single cell level (Gaglia et al., 2020). A recent mammalian study discovered the existence of both HSF1 nSBs at non-*hsp* gene loci and smaller HSF1 condensates at transcriptionally active *hsp* gene loci upon heat shock (H. Zhang et al., 2022). In this study, HSF1 in the smaller condensates was found to colocalize with transcription apparatus factors, including RNA Pol II, BRD4, MED1, and CYCT1 (H. Zhang et al., 2022). It is thus possible that upon heat shock, HSF1 in nSBs sequesters transcription factors to halt general transcription, while HSF1 in the smaller condensates functions to induce the transcription of *hsp* target genes. HSF1 nSBs that are not able to resolve may go on to transition from liquid to gel phase condensates, which could then permanently hinder HSF1 activity and the HSR. Our study did not analyze small HSF-1 condensates, and it is not yet known if these are present in the worm. However, we found that *cbp-1* knockdown promotes the recovery of large HSF-1 nSBs after heat shock. Thus, CBP-1 may facilitate the stabilization of HSF-1 nSBs, which could promote the gel phase state upon prolonged stress, leading to ultimate HSF-1 inactivation. We hypothesize that the removal of CBP-1 through RNAi could thus enhance the HSR. We do not know how CBP-1 may stabilize HSF-1 nSBs. It could be through the acetylation of HSF-1 or

another protein, through providing a scaffolding, or through an alternative mechanism. It will be interesting to investigate these possibilities in future work.

CBP-1 also functions as a regulator of multiple other stress response pathways. Interestingly, CBP-1 positively regulates SKN-1/Nrf activation and the oxidative stress response, where it regulates SKN-1 activity and protein abundance (Ganner et al., 2019). CBP-1 is also an essential regulator of the mitochondrial unfolded protein response (T. Y. Li et al., 2021). Collectively, our studies identify a new role of CBP-1 in HSR regulation in *C. elegans* and its physiological effects at the organismal level. CBP-1 negatively regulates HSP expression, nuclear stress body recovery, and thermotolerance ability of the worm. Future work is needed to determine the precise mechanism of action of CBP-1 in the HSR pathway and any potential acetylation changes of HSF-1 that are induced by CBP-1.

A

Human KATs	*C. elegans* Homolog
P300 (KAT3B)	CBP-1
ACAT1	KAT-1
HAT1 (KAT1)	HAT-1
TAF1 (KAT4)	TAF-1
KAT5	MYS-1
MYST1 (KAT8)	MYS-2
MYST3 (KAT6A)	MYS-4
MYST3 (KAT6A)	LSY-12
ATAT1	MEC-17
GCN5 (KAT2A)	PCAF-1
ATAT1	ATAT-2
ACAT1	T02G5.4

B

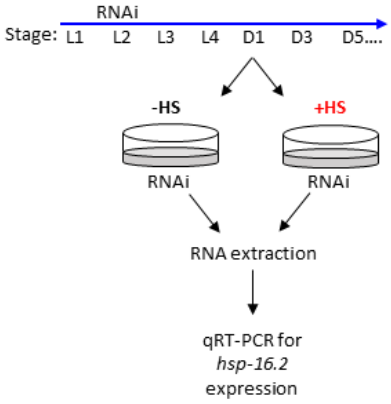

C

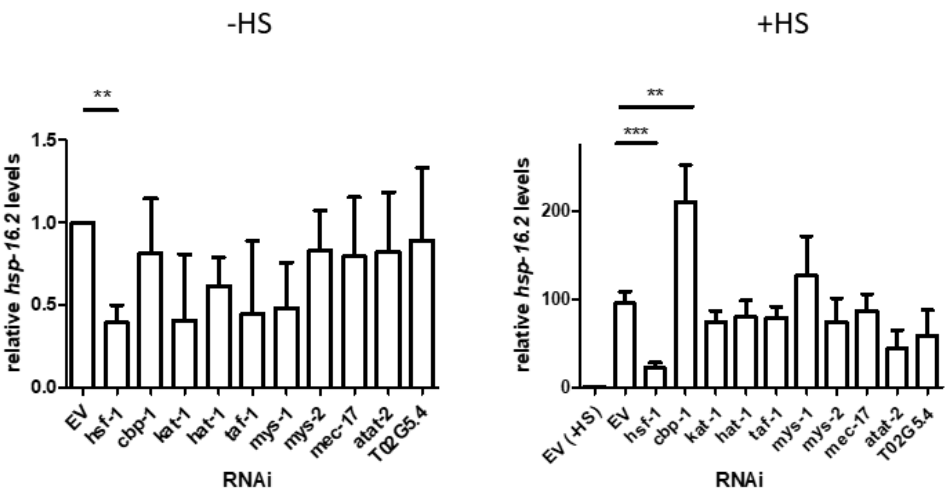

Figure 2.1: Targeted-RNAi screen for lysine acetyltransferase modulators of the HSR identifies CBP-1. A) Table of all putative lysine acetyltransferases (KATs) and their human homologs. **B)** Schematic of the targeted RNAi screen for lysine acetyltransferase modulators of the HSR. ~75% of worm KATs were screened by examining endogenous *hsp-16.2 gene expression*, a heat-inducible heat shock protein gene, before and after heat shock using qRT-PCR. **C)** N2 (wildtype) animals were fed empty vector (EV) control or KAT RNAi from 19 hrs after L1 larval stage to Day 1 of adulthood. RNA was extracted from Day 1 animals before and immediately after a 1-hour heat shock at 33ºC and *hsp-16.2* levels were quantified by qRT-PCR using the ΔΔCt method (n=3 biologically independent samples). The housekeeping gene cdc-42 (R07G3.1) was used for normalization. Statistical analysis was determined by conducting a One-Way ANOVA using GraphPad Prism (GraphPad Software, www.graphpad.com) followed by a Tukey post hoc test comparison of all columns. *p-value < 0.05, **p-value < 0.01, ***p-value < 0.001.

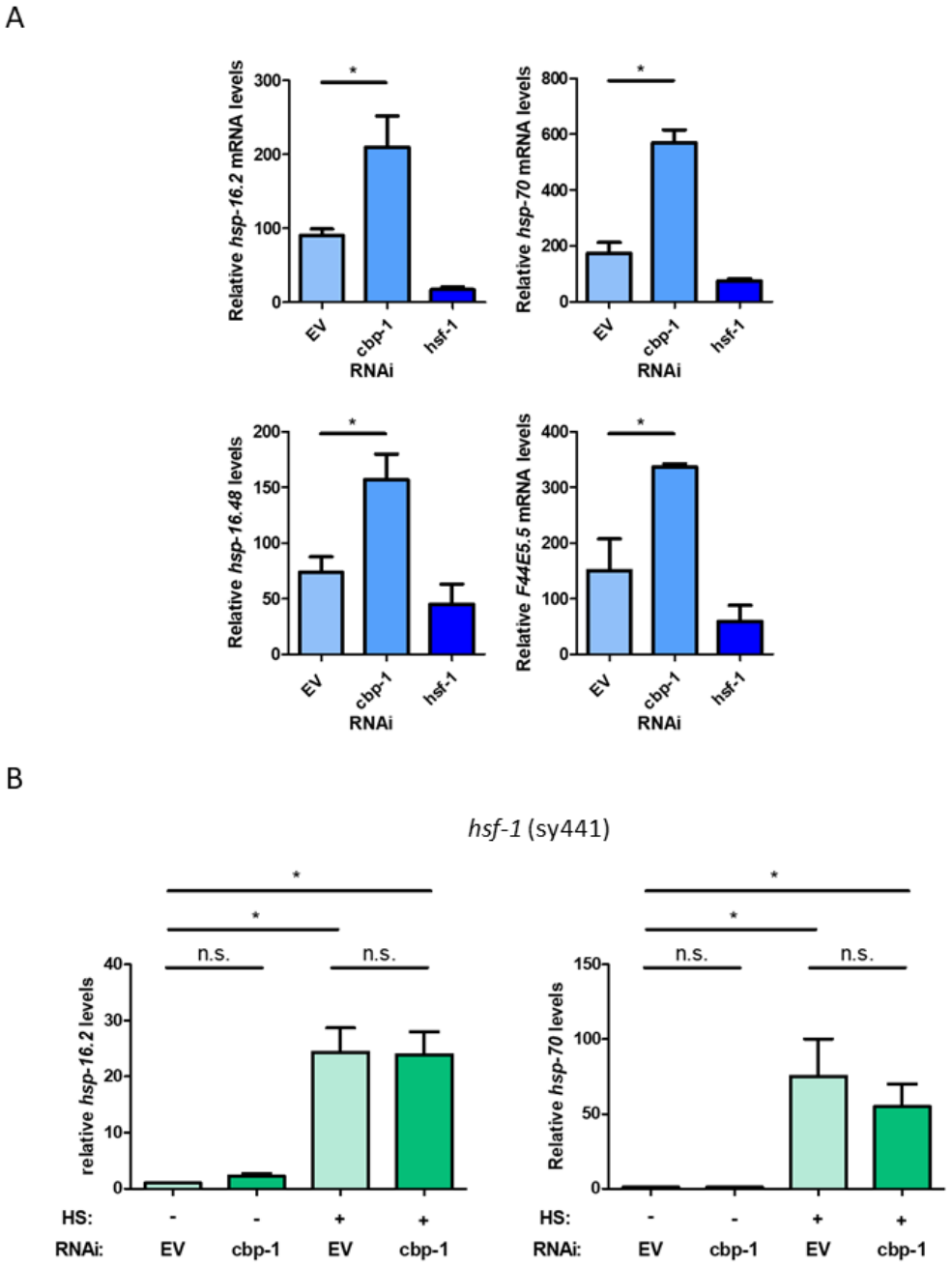

Figure 2.2: CBP-1 regulates the expression of multiple HSF-1 target genes in an HSF-1-dependent manner. A) RNA was extracted from N2 (wildtype) worms on Day 1 of adulthood with a 1-h heat shock at 33°C that were fed empty vector (EV), *cbp-1*, or *hsf-1* RNAi beginning 19 h after L1. Heat shock inducible heat shock protein gene expression levels for *hsp-16.2*, *hsp-16.48*, *F44E5.5*, and *hsp-70* were quantified by qRT-PCR. **B)** RNA was extracted from an HSF-1 deletion worm strain (PS3551) on Day 1 of adulthood with and without a 1-h heat shock at 33°C with animals fed EV or *cbp-1* RNAi. PS3551 animals were fed empty vector (EV) control or *cbp-1* RNAi from 19 h after L1 larval stage to Day 1 of adulthood. Heat shock inducible *hsp-16.2* and *hsp-70* levels were quantified by qRT-PCR. Statistical analysis was determined by determined by conducting a One-Way ANOVA using GraphPad Prism (GraphPad Software, www.graphpad.com) followed by a Tukey post hoc test comparison of all columns. *p-value < 0.05.

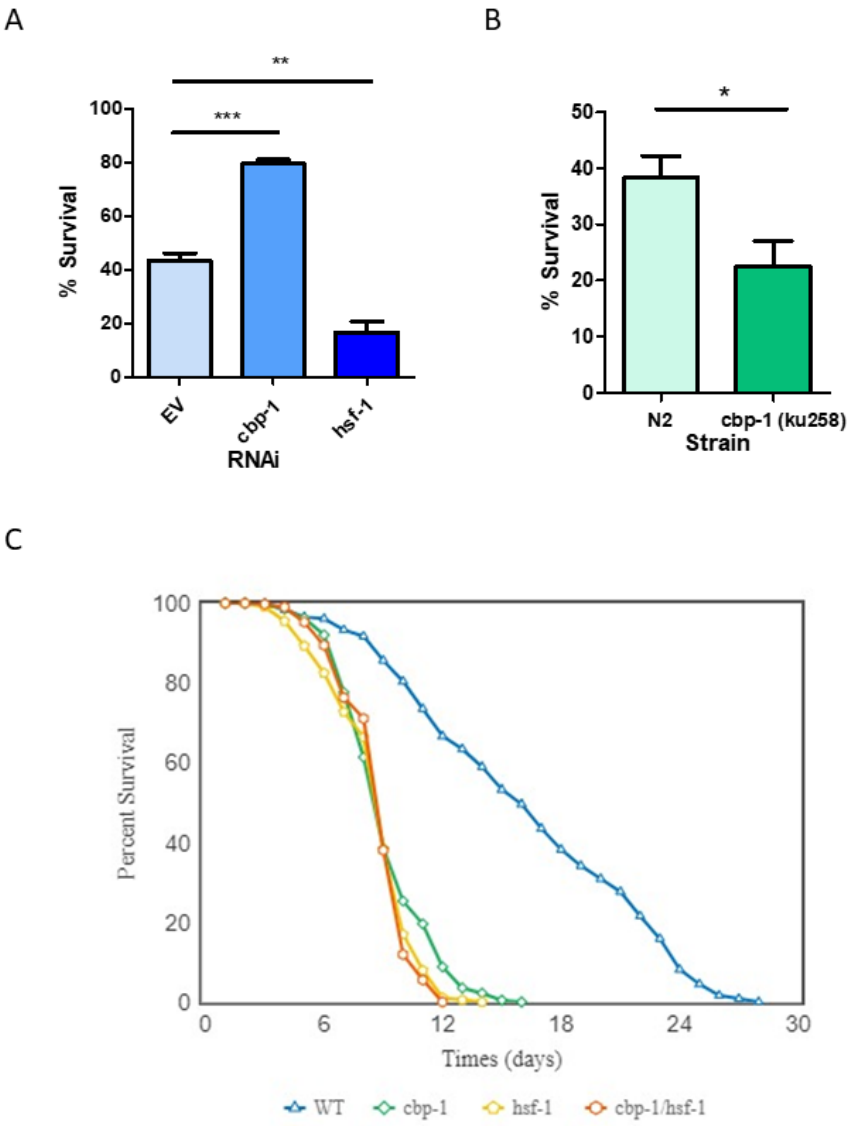

Figure 2.3: Effect of CBP-1 on thermotolerance and lifespan. A) In order to assess CBP-1 activity on resistance to heat stress, N2 worms were given a lethal heat shock of 3.5 h at 37°C on Day 1 of adulthood and then ~ 100 animals were randomly scored for survival after a 48-h recovery. Percent survival was determined for worms fed with empty vector (EV), *cbp-1*, and *hsf-1* RNAi. Data was plotted as % survival using GraphPad Prism (GraphPad Software, www.graphpad.com) and was analyzed with a two-tailed t test. *p-value < 0.05, **p-value < 0.01, ***p-value < 0.001. **B)** Thermotolerance was assessed in N2 and SDW173, a strain containing a gain-of-function allele of *cbp-1* that increases acetyltransferase activity (MH2430 strain outcrossed 3x to N2). Data was plotted as % survival using GraphPad Prism (GraphPad Software, www.graphpad.com) and was analyzed with a two-tailed t test. *p-value < 0.05. **C)** Lifespan analysis was performed in wild type N2 animals fed with EV, *cbp-1* RNAi, *hsf-1* RNAi, or *cbp-1/hsf-1* double RNAi throughout the lifespan. Worms were scored approximately every day for survival. The average survivability of three replicates was plotted using OASIS 2 (https://sbi.postech.ac.kr/oasis2/) (Han et al., 2016), and statistical analysis was done by Log-rank (Mantel-Cox) Test (Shown in Appendix A1).

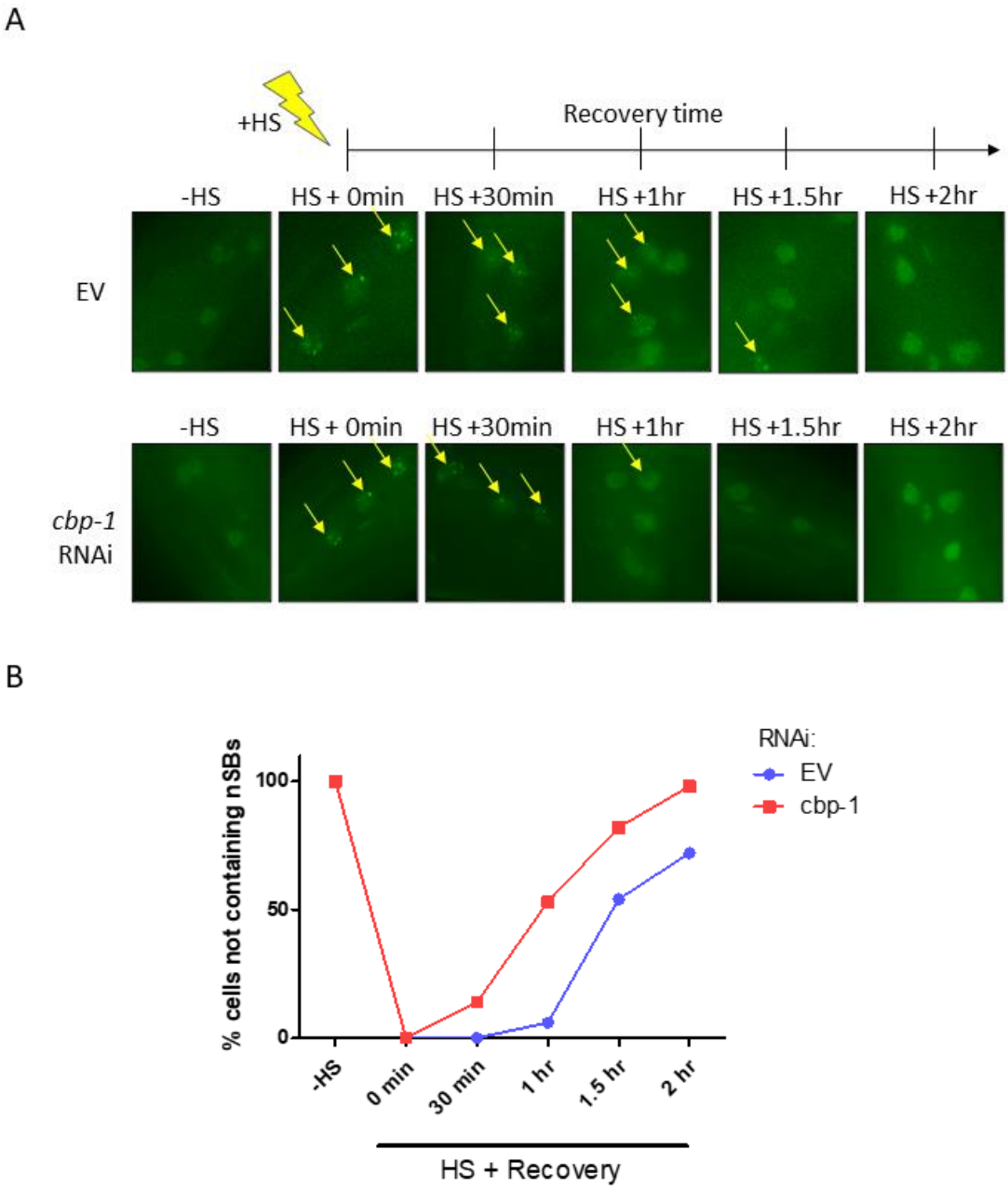

Figure 2.4: cbp-1 RNAi increases recovery rate of nuclear stress bodies (nSBs) after heat shock. A) Fluorescent images of HSF-1:GFP in the SDW015 strain were examined before heat shock and in 30-min increments after a 15-min heat shock at 33°C for 2 h at 20°C until the majority of hypodermal cells containing nuclear stress bodies (nSBs) had been resolved. Images represent fluorescent nSB formation in hypodermal cells under control and *cbp-1* RNAi conditions at each time point in Day 2 adult worms. Yellow arrows indicate hypodermal cell nuclei containing nSB foci. **B)** The percentage of hypodermal cells not containing nSBs were quantitated following fluorescent imaging of worms fed empty vector (EV) control and *cbp-1* RNAi (n = 10 worms). Significance was determined using 2-way ANOVA. Column *p-value = 0.0497; row **p-value = 0.0022.

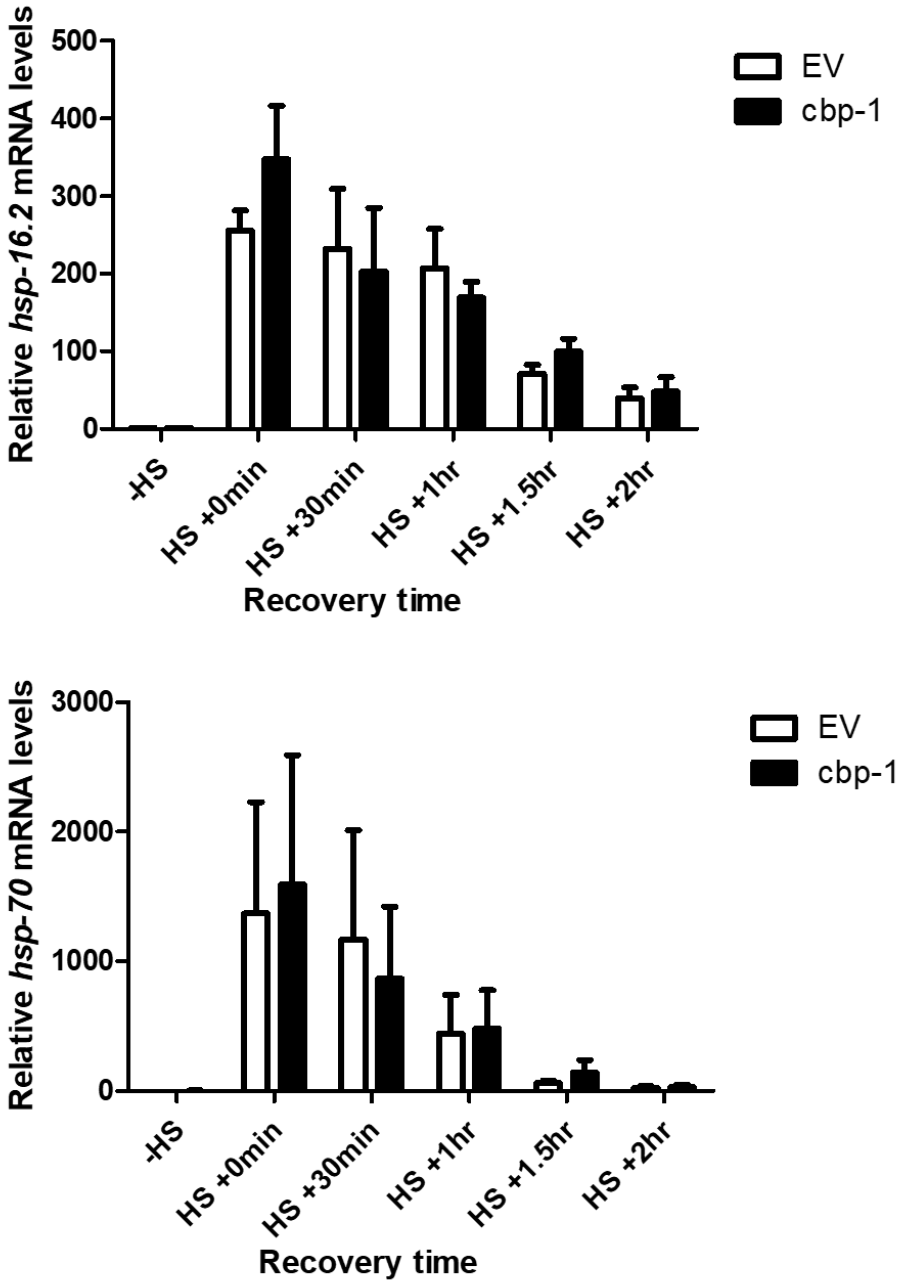

Figure 2.5: *cbp-1* RNAi does not alter expression kinetics of *hsp-16.2* or *hsp-70* expression after heat shock. RNA was extracted from wildtype (N2) worms on Day 1 of adulthood that were fed empty vector (EV), *cbp-1*, or *hsf-1* RNAi beginning 19 hrs after L1. *hsp-16.2* and *hsp-70* levels were quantified by qRT-PCR (n=3 biologically independent samples). Statistical analysis determined by determined by conducting a One-Way ANOVA using GraphPad Prism (GraphPad Software, www.graphpad.com) followed by a Tukey post hoc test comparison of all columns. *p-value < 0.05.

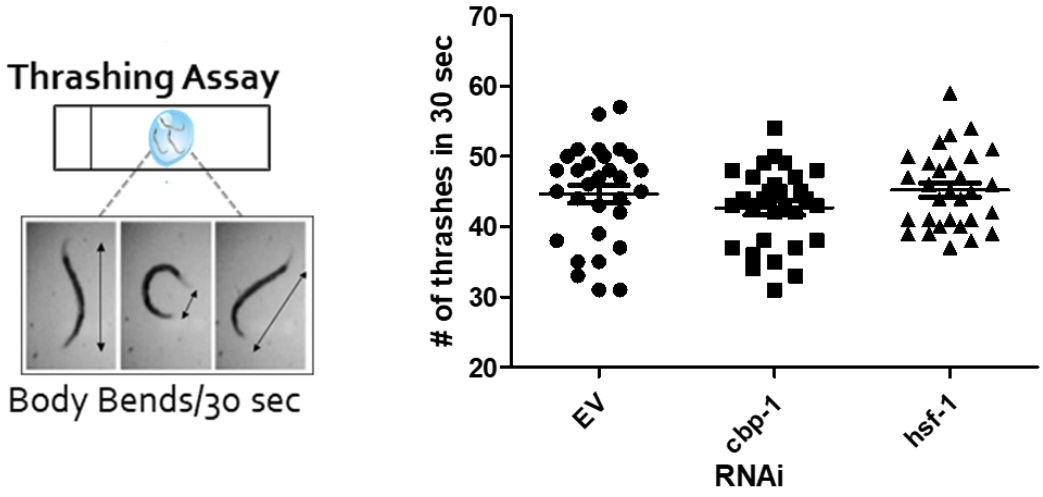

Figure 2.6: *cbp-1* RNAi does not alter motility. Motility of the N2 wildtype strain under control EV, *cbp-1*, or *hsf-1* RNAi was measured by placing the worms in a drop of NGM buffer and counting the number of thrashes in 30 seconds after a 1-minute recovery period (n=~15 worms). Thrashing assay was conducted in biological triplicate and statistics were analyzed using GraphPad Prism (GraphPad Software, www.graphpad.com) and was analysed with a two-tailed t test. *p-value < 0.05.

CHAPTER THREE: REGULATION OF THE HEAT SHOCK RESPONSE IN NEURODEGENERATIVE DISEASES IN *C. ELEGANS*

Abstract

Defects in proteostasis that occur with aging are central to many human diseases, including Alzheimer's disease, Parkinson's disease, and Huntington's disease. These neurodegenerative diseases (NDDs) are proteotoxic diseases hallmarked by increased protein misfolding and aggregation. Many components of the heat shock response, a cellular stress response that refolds misfolded or aggregating proteins to maintain proteostasis, are downregulated in NDD and aging, including the transcription factor Heat Shock Factor 1 (HSF1) that controls this stress response. The regulation of HSF-1, the *C. elegans* homolog of HSF1, in neurodegenerative diseases has yet to be fully elucidated. Thus, we examined regulation of HSF-1 and its target genes in NDD models in *C. elegans.* We found that *hsf-1* expression is decreased in an Alzheimer's disease model expressing human amyloid-β1-42 (Aβ). In contrast, we found that the presence of Aβ increased the expression of heat shock inducible HSF-1 target genes *hsp-16.2* and *hsp-70*. To further examine the relationship between HSF-1 and Aβ, we utilized an endogenous HSF-1::GFP worm strain previously made in the lab that we then crossed with the Aβ model of Alzheimer's disease to visualize tissue-specific HSF-1 expression in the disease state and with age. We visualized HSF-1::GFP foci in multiple tissue types in the Aβ background. Collectively, these findings begin uncovering the regulation of HSF-1 and the heat shock response in neurodegenerative disease in *C. elegans*.

Introduction

Neurodegenerative diseases, such as Alzheimer's disease, Huntington's disease, and Parkinson's disease, are considered proteotoxic diseases associated with an increase in protein misfolding or aggregation (Muchowski & Wacker, 2005). The protein toxicity of these neurodegenerative diseases leads to neuronal dysfunction and subsequent neuronal death, causing various symptoms for patients from dementia to tremors. Huntington's disease is hallmarked by the abnormal polyglutamine expansion in the Huntingtin protein in the N-terminal domain. These polyglutamine expansions can aggregate together causing large inclusion bodies of aggregating Huntingtin protein (Havel et al., 2009). Alzheimer's disease results from the aggregation of the toxic protein amyloid-β. The accumulation and aggregation of this protein causes neuronal loss in the brain leading to dementia or loss of cognition (Mavroudis et al., 2010). Parkinson's disease is hallmarked by the aggregation of the protein alpha-synuclein that form Lewy bodies and leads to loss of dopaminergic neurons in the brain (E. Kim et al., 2016).

Protein toxicity disrupts the proteostasis in the cell that is needed for its proper function (Labbadia & Morimoto, 2015). Current drug treatments of these neurodegenerative diseases combat the symptoms associated with these diseases but not the underlying proteotoxicity causing these symptoms (Gomez-Pastor et al., 2018). Therefore, novel therapeutic drugs are currently needed to treat these diseases and the underlying proteostasis dysfunction caused by the proteotoxicity of the protein aggregates. Studies in the heat shock response have demonstrated therapeutic potential in enhancing the protein folding capacity of cells (Neef et al., 2011).

The HSR is a key player in the proteostasis network, known to play a role in a variety of physiological processes, including development, reproduction, aging, and age-related diseases (Joutsen & Sistonen, 2019). The HSR is a highly conserved cellular response that maintains

proteostasis in the cell through the activation of heat shock transcription factor 1 (HSF1). HSF1 is the master regulator of the HSR and when activated, drives the expression of heat shock proteins (HSPs) that act as molecular chaperones to restore proteostasis after stress (Hartl et al., 2011). The decline of HSF1 activity in aging and in neurodegenerative diseases have been well documented (Anckar & Sistonen, 2011). For example, in patients with Alzheimer's disease, Purkinje cells show depleted levels of HSF1 and HSPs (Jiang et al., 2013). Similarly, overexpression of HSF1 lowers amyloid-β levels in Purkinje cells and decreases the cognitive impairment associated with Alzheimer's (Pierce et al., 2013). Previous studies have also shown that HSF1 levels and HSP levels are depleted in Huntington's disease and Parkinson's disease patient brains (Gomez-Pastor et al., 2017; Jiang et al., 2013; E. Kim et al., 2016).

The activity of HSF-1, the *C. elegans* homolog of HSF1, is highly conserved and makes *C. elegans* a useful model organism to study the regulation of HSF-1 during stress and disease. In this study, we utilized *C. elegans* to examine the regulation of the HSR in neurodegenerative disease. We discovered that *hsf-1* expression is decreased in the presence of amyloid-β1-42, especially in aging. However, conversely, we found that HSF-1 target gene expression was increased under the same conditions. Thus, we created a worm strain to visualize HSF-1 levels in the Alzheimer's disease model to examine the effect of amyloid-β1-42 on HSF-1 protein levels to better understand the mechanism behind the decline in the HSR in the Alzheimer's background. Collectively, understanding how HSF1 is being regulated in neurodegenerative disease could provide insight into novel therapeutics to reduce or prevent the protein aggregation associated with neurodegenerative disease.

Methods

C. elegans strains and maintenance

The following strains were used in this study: N2 (Bristol), CL2006 - dvIs2 (pCL12(unc-54/human Abeta peptide 1-42 minigene) + rol-6(su1006)), AM140 - rmIs132 (unc-54p::Q35::YFP), NL5901 - pkIs2386 (unc-54p::alphasynuclein::YFP + unc-119(+)), SDW015 - *hsf-1*(asd002(*hsf-1::GFP* + *unc-119*(+)), and SDW068. The SDW068 strain was created by genetically crossing CL2006 with SDW015. Strains were maintained at 20°C on standard NGM plates seeded with *Escherichia coli* OP50-1. The synchronous population of nematodes was obtained by bleach synchronization and plated for 19 hrs on NGM plates without food.

RNA isolation and quantitative PCR

RNA was extracted with TRIzol® reagent (Ambion®, cat# 15,596–026) by standard protocol. RNA was reverse transcribed using a High Capacity cDNA Reverse Transcription Kit (Applied Biosystems, cat# 4,368,814). cDNA was diluted to 100 ng/µl to be used as a template for qRT–PCR performed with the StepOne Plus Real-time PCR system (Applied Biosystems, cat # 4,376,600) using iTaq™ Universal SYBR® Green Supermix (Bio-Rad, cat# 1,725,121) according to the manufacturer's instructions. Expression levels were analyzed via qPCR using the ΔΔCt method. The housekeeping gene *cdc-42* (R07G3.1) was used for normalization. Results show averages of independent biological triplicates performed in technical triplicates. Statistical analysis was performed with GraphPad (GraphPad Software, https://www.graphpad.com) using an unpaired Student’s t-test.

Primers used: *hsf-1* (Y53C10A.12) Fwd: TGCAGCCAGGATTGTCGA, Rvs: GGCGGCGCAAAAGTCTATT; *hsp16.2* (Y46H3A.3) Fwd: ACGCCAATTTGCTCCAGTCT,

Rvs: TGATGGCAAACTTTTGATCATTGT; *hsp-70* (C12C8.1) Fwd: TTCAATGGGAAGGACCTCAACT, Rvs: GGCTGCACCAAAGGCTACTG; *cdc-42* (R07G3.1) Fwd: CTTCTGAGTATGTGCCGACAGTCT, Rvs: GGCTCGCCACCGATCAT

Fluorescent microscopy

Fluorescent images were obtained using a Keyence BZ-X fluorescent microscope. Animals were picked free of bacteria and anesthetized with 10 mM levamisole. Worms containing HSF-1::GFP were examined in all tissue types HSF-1::GFP is present, including hypodermal, muscle, intestinal, and germline cells (Deonarine et al., 2021).

Statistical analyses

Statistical analyses were carried out with GraphPad Software (GraphPad Software, La Jolla, CA, USA, https://www.graphpad.com) unless otherwise stated. All error bars are representative of standard deviation between independent biological replicates, as indicated.

Results

hsf-1 mRNA expression decreased in Alzheimer's disease model but not Huntington's disease or Parkinson's disease models

Previous studies have found HSF-1 levels to be decreased in the presence of alpha-synuclein and polyglutamine expansions in cell lines expressing these proteins. To examine the effects of neurodegenerative disease aggregate formation on the heat shock response in *C. elegans*, we utilized three widely used models of neurodegenerative disease: CL2006 - an Alzheimer's disease model, AM140 – a Huntington's disease model, and NL5901 – a Parkinson's disease model. The Alzheimer's model, strain CL2006, expresses a human 42-amino acid beta-amyloid

(Aβ1-42) peptide using a muscle-specific promoter. It forms Aβ protein aggregates with age causing paralysis of the worm (Link, 1995). The Huntington's model, strain AM140, expresses one polyglutamine (polyQ) expansion of 35 glutamine residues of the Huntingtin protein using a muscle-specific promoter tagged with YFP (Q35::YFP) (Cornaglia et al., 2016). These Q35::YFP worms transition from soluble polyglutamine expression to aggregating polyglutamine expression with age (Cornaglia et al., 2016). The Parkinson's model, strain NL5901, contains human alpha-synuclein tagged with YFP that aggregates in the muscle with age (van Ham et al., 2008).

We examined *hsf-1* mRNA levels in these neurodegenerative disease models to determine if the presence of aggregate formation affects its expression. We isolated RNA from Day 1 and Day 6 adults in N2 (wildtype), CL2006, AM140, and NL5901 strains and measured expression of *hsf-1* using RT-qPCR. We found that only in the Alzheimer's model, CL2006, was there a significant decrease in *hsf-1* mRNA compared to wildtype on Day 1 of adulthood (Figure 3.1). We found that levels of *hsf-1* normally decrease with age in wildtype conditions; however, the levels of *hsf-1* remained consistent with age in all of the neurodegenerative disease models (Figure 3.1). Overall, the levels of *hsf-1* were decreased in the presence of Aβ but not in the presence of polyQ or α-synuclein.

HSP mRNA levels increase in Alzheimer's and Huntington's models but not Parkinson's model

To further examine the role of NDD aggregate formation on the HSR, we examined how the neurodegenerative disease models affects the heat shock inducible HSF-1 target genes *hsp-16.2* and *hsp*-70 using qRT-PCR. We found that both *hsp-16.2* and *hsp-70* expression was significantly increased in the Alzheimer's disease model compared to wildtype (Figure 3.2). *hsp-70* expression levels were also significantly increased in the Huntington's disease model;

however, *hsp-16.2* levels were similar to wildtype (Figure 3.2). On the other hand, the Parkinson's disease model had no effect on *hsp* expression levels (Figure 3.2).

Visualization of HSF-1 in wildtype and Alzheimer's disease background

Since we found significant changes to *hsf-1* and HSP expression in the Alzheimer's disease model, we next wanted to visualize HSF-1 changes in the worm at the tissue level in the presence of Aβ1-42. The Aβ1-42 aggregates form in only the muscle cells. Thus, we wanted to determine tissue-specific HSF-1 changes with age in this model. To visualize HSF-1 protein levels, we utilized an HSF-1::GFP strain, SDW015, created previously in the lab. With this strain we are able to easily visualize HSF-1 in all tissue types, including muscle cells (Deonarine et al., 2021). We genetically crossed the HSF-1::GFP strain with the Alzheimer's disease model, CL2006 (Fay, 2006) to create the SDW068 strain. We utilized fluorescent microscopy to identify HSF-1::GFP in all cell types, including muscle, intestinal, and germline cells, in the Aβ1-42 Alzheimer's disease background (Figure 3.3). Here we found that HSF-1::GFP was present in all tissue types including the muscle cells where the amyloid-beta forms. Further investigation of the quantification of HSF-1::GFP in the muscle cells with and without the presence of amyloid-beta would be needed. Examining HSF-1::GFP levels with age in wildtype and the amyloid-beta background would be beneficial as the Aβ1-42 aggregates form with age.

Discussion

We sought to elucidate the effect of neurodegenerative disease on HSF-1 and HSP expression in *C. elegans*. Here, we examined *hsf-1* mRNA expression in an Alzheimer's disease, Huntington's disease, and Parkinson's disease model. We found that only in the presence of amyloid-beta in the Alzheimer's disease model did *hsf-1* expression decrease. In contrast, we found that both the

Alzheimer's model and the Huntington's model had increased HSP expression. To further examine this regulation of HSF-1 and the HSR, we created a HSF-1::GFPxAβ1-42 strain to examine HSF-1 levels in the presence of amyloid-beta using fluorescent microscopy. Overall, these studies suggest that neurodegenerative disease protein aggregation regulations HSF-1 and HSR activity.

Our data suggests that *hsf-1* gene expression is downregulated in the presence of amyloid-beta in an Alzheimer's disease model. Here we utilized whole-worm RNA isolation, but it would be interesting to examine tissue-specific gene expression solely in tissues expressing the protein aggregates. Understanding how HSF-1 is affected by the presence of neurodegenerative disease protein aggregates at this level will give a better insight into its regulation of the HSR. Examining HSF-1 regulation at the protein level would also help determine the mechanism of neurodegenerative disease regulation. In mammals, the downregulation of HSF1 in neurodegenerative disease is at the protein level (Gomez-Pastor et al., 2017; E. Kim et al., 2016). Utilizing the created HSF-1::GFPxAβ1-42 strain (SDW068) can provide more insight into this regulation in *C. elegans*.

While we found *hsf-1* gene expression to be downregulated in the Alzheimer's disease model, we found that HSF-1 target genes *hsp-16.2* and *hsp-70* gene expression to be unregulated. This conflict suggests that further research be performed to identify the kinetics of active HSF-1 and if there are potentially other mechanism by which HSPs are being activated. It is possible that other transcription factors can also activate HSPs. It will be insightful to identify if these alternative pathways for HSP induction are being utilized as *hsf-1* gene expression is being suppressed. Overall, further studies are needed to determine the precise mechanism behind neurodegenerative disease regulation on the HSR in *C. elegans*.

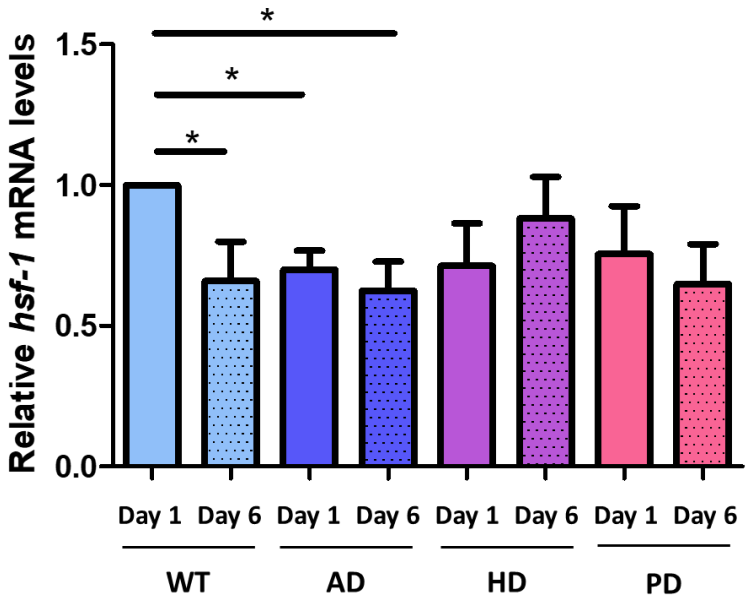

Figure 3.1: *hsf-1* mRNA expression decreased in Alzheimer's disease model but not Huntington's disease or Parkinson's disease models. RNA was extracted from wildtype (N2), Alzheimer's model (AD) (CL2006), Huntington's model (HD) (AM140), and Parkinson's model (PD) (NL5901) worms on Day 1 and Day 6 of adulthood. *hsf-1* mRNA levels were quantified by quantitative RT-PCR (n=3 biologically independent samples). Statistical analysis was determined by determined by conducting a One-Way ANOVA using GraphPad Prism (GraphPad Software, www.graphpad.com) followed by a Tukey post hoc test comparison of all columns. *p-value < 0.05.

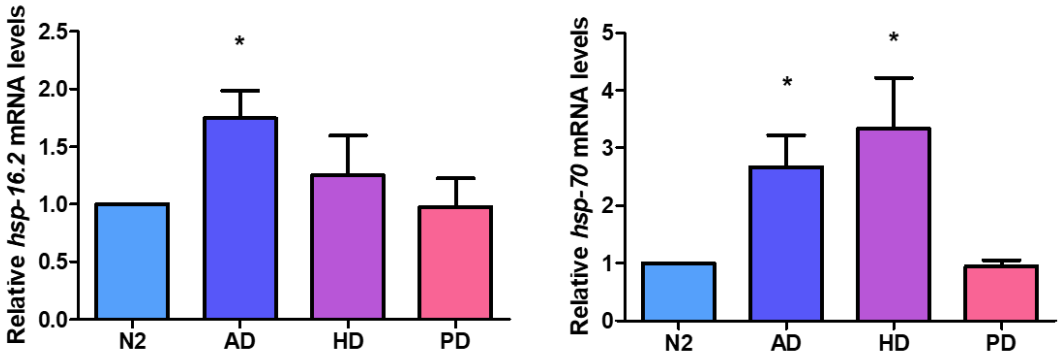

Figure 3.2: HSP mRNA levels increase in Alzheimer's and Huntington's models but not Parkinson's model. RNA was extracted from wildtype (N2), Alzheimer's model (CL2006), Huntington's model (AM140), and Parkinson's model (NL5901) worms on Day 3 of adulthood. *hsp-16.2* and *hsp-70* levels were quantified by RT-PCR (n=3 biologically independent samples). Statistical analysis was determined by determined by conducting a One-Way ANOVA using GraphPad Prism (GraphPad Software, www.graphpad.com) followed by a Tukey post hoc test comparison of all columns. *p-value < 0.05.

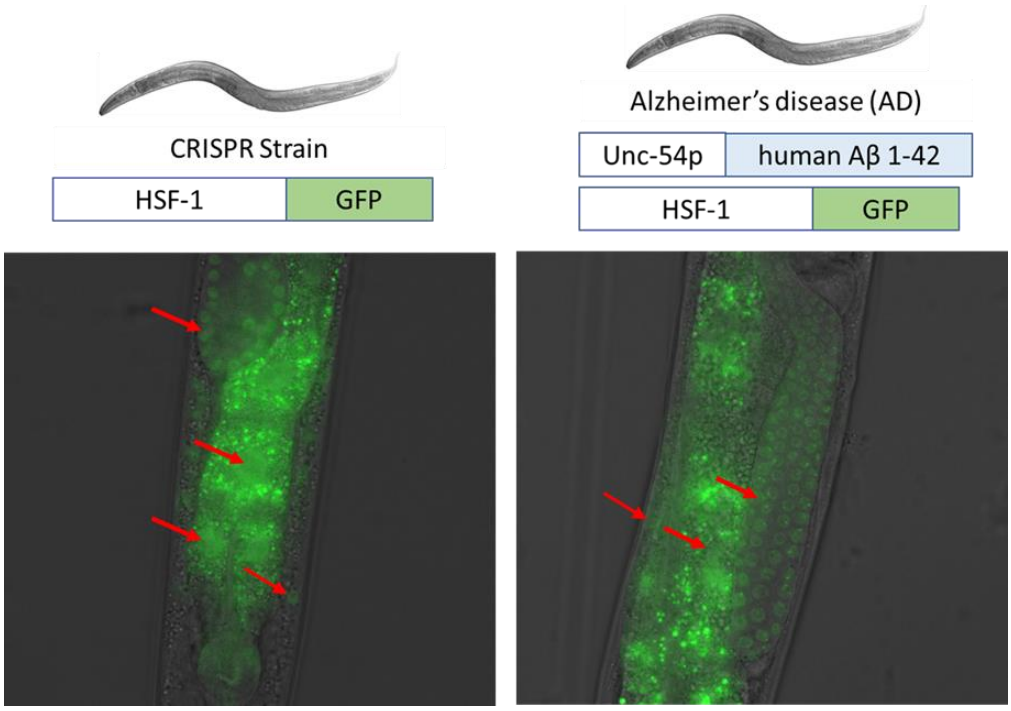

Figure 3.3: Visualization of HSF-1 in wildtype and neurodegenerative disease background. A CRISPR strain containing HSF-1 tagged with GFP at its endogenous locus (SDW015) was crossed with the Aβ42 Alzheimer's disease model (CL2006). Levels of HSF-1 in wildtype worms and in the AD model were imaged on Day 3 adults. Select cells expressing HSF-1::GFP are marked with arrows including muscle, intestinal, and germline cells.

CHAPTER FOUR: HSF-1 DEGRADATION VIA E3 LIGASE REGULATION IN NEURODEGENERATIVE DISEASE IN *C. ELEGANS*

Abstract

The mechanism of HSF1 degradation in general, and in neurodegenerative disease in particular, is not thoroughly characterized. Recent studies have identified two E3 ubiquitin ligases, FBXW7 and NEDD4, that target HSF1 for degradation in Huntington's and Parkinson's disease, respectively. Our goal is to further elucidate the mechanism of HSF1 degradation in neurodegenerative disease using *C. elegans* models. We have found that knockdown of the *C. elegans* homologs for FBXW7 and NEDD4, *sel-10* and Y92H12A.2, does not alter HSP reporter, *hsp-16.2*p::GFP and *hsp-70*p::GFP, activity in the wildtype background. However, we also examined E3 ligase knockdown in a Huntington's disease model that expresses polyglutamine expansions with age. In this neurodegenerative disease background, we found that *sel-10* and Y92H12A.2 RNAi increased motility and thermotolerance. Thus, both E3 ligases only regulate the HSR in the presence of polyglutamine expansions. These studies provide more knowledge on the regulation of HSF-1 in neurodegenerative disease, specifically Huntington's disease, and a potential mechanism for the decrease in HSR activity in the presence of proteotoxic aggregate formation.

Introduction

The heat shock response is a highly conserved cellular response to stressors that disrupt the proteostasis of the cell. Stressors such as heat shock, heavy metals, and oxidative stress can activate the heat shock response (HSR) (Labbadia & Morimoto, 2015). Genes encoding for molecular chaperones are induced by heat shock transcription factor 1 (HSF1) and aid in the re-folding or degradation of damaged proteins. Upon stress, HSF1 trimerizes and induces transcription of molecular chaperones, including heat shock proteins (HSP) HSP70, HSP90, and HSP60 (Figure 1) (Westerheide et al., 2009). These heat shock proteins guide protein folding and degradation to equilibrate the proteostasis of the cell. Upon attenuation, HSF1 is degraded by the ubiquitin-proteasome system (Kourtis, Moubarak, et al., 2015). The transcriptional activity of HSF1 is stress inducible and highly regulated (Westerheide et al., 2012). The HSR is known to play a role in a variety of physiological processes, including development, reproduction, aging, and age-related diseases (Joutsen & Sistonen, 2019). HSF1 has been implicated in a wide array of age-related diseases, including neurodegenerative diseases, metabolic diseases, and cancer (Gomez-Pastor et al., 2018). Understanding HSF1 regulation with aging may be useful when developing therapeutic strategies for such diseases.

It has been widely documented that HSF-1 and heat shock protein activity is impaired in aging and neurodegenerative diseases (Anckar & Sistonen, 2011). Downregulation of the heat shock response in these protein misfolding diseases contributes to the protein aggregation and overall neuronal dysfunction and death (Gomez-Pastor et al., 2017). Many studies have found that upregulating HSF1 or HSP activity has beneficial effects on the proteotoxicity of the diseases (Neef et al., 2011). Previous studies have shown that HSF1 levels and HSP levels are depleted in Alzheimer's, Huntington's, and Parkinson's disease patient brains (Gomez-Pastor et al., 2017;

Jiang et al., 2013; E. Kim et al., 2016). In Huntington's and Parkinson's disease, the depletion of HSF1 is due to its degradation. Abnormal degradation of HSF1 in Huntington's was found to be mediated by proteasomal degradation via the E3 ligase FBXW7 (Gomez-Pastor et al., 2017). Similarly, HSF1 phosphorylation at S303 and S307 was found to mediate this degradation by FBXW7. HSF1 phosphorylation was found to be modified by Casein Kinase 2 (CK2). Both CK2 and FBXW7 are upregulated in Huntington's disease (Gomez-Pastor et al., 2017). HSF1 degradation in Parkinson's disease was found to involve the E3 ligase NEDD4, which is upregulated in the diseased patients (E. Kim et al., 2016). Ultimately, the role of HSF1 degradation under basal conditions as well as in neurodegenerative disease has not been fully elucidated.

Proteins needing to be sent for degradation to the proteasome are tagged with ubiquitin that is recognized by the proteasome and where a series of enzymatic reactions is used to degrade the targeted protein (Wang & Le, 2019). The process of ubiquitination is comprised of three enzymes: the E1 enzyme that activates ubiquitin, the E2 molecule that binds to the ubiquitin, and the E3 ligase that transfers the ubiquitin from the E2 molecule to the targeted protein. There are hundreds of E3 ligases that bind to specific substrates for ubiquitin transfer (Wang & Le, 2019). In the case of HSF1, only FBXW7 and NEDD4 are known to ubiquitinate HSF1 in the presence of disease protein aggregation (Gomez-Pastor et al., 2017; E. Kim et al., 2016).

The activity of HSF-1, the *C. elegans* homolog of HSF1, is highly conserved and makes *C. elegans* a useful model organism to study the regulation of HSF-1 during stress and disease. Similarly, E3 ligases and the ubiquitin-proteasome system are highly conserved in *C. elegans* (Papaevgeniou & Chondrogianni, 2014). In this study, we utilized *C. elegans* to examine E3 ligase regulation of the HSR in neurodegenerative disease, specifically Huntington's disease. We

identified a role for SEL-10 and Y92H12A.2 in negatively regulating the HSR, via motility and thermotolerance ability, in a Huntington's disease model in *C. elegans*, confirming the importance of these regulators in this stress response pathway. Collectively, our studies demonstrate a potential novel role for E3 ligase regulation of the HSR in neurodegenerative disease.

Methods

C. elegans strains and maintenance

The following strains were used in this study: N2 (Bristol), TJ375 - gpIs1 (hsp-16.2p::GFP), AM446 - (hsp-70p::GFP), and AM140 - rmIs132 (unc-54p::Q35::YFP). Strains were maintained at 20°C on standard NGM plates seeded with *Escherichia coli* OP50-1. The synchronous population of nematodes was obtained by bleach synchronization and plated for 19 hrs on NGM plates without food.

RNA interference

Synchronous L1 nematodes were grown on standard NGM plates seeded with OP50-1 bacteria for 19 hrs to prevent potential RNAi-mediated effects on early development. Worms were transferred onto standard NGM plates supplemented with 25 µg/ml carbenicillin and 1 mM isopropyl-beta-ᴅ-thiogalactopyranoside (IPTG) and seeded with either HT115 bacteria containing an empty vector (EV/L4440 control) or with sequence-verified gene-specific RNAi strains isolated from the Ahringer RNAi library (J. Ahringer, University of Cambridge, Cambridge, U.K.), as previously described (Kamath et al., 2003). To induce dsRNA production, HT115 bacteria were supplemented with 1 mM IPTG shaking at 37°C for 1 hour before seeding.

Fluorescent microscopy and GFP analysis

Transgenic worms containing the fluorescent reporter (TJ375 and AM446) were synchronized, plated on RNAi plates from L1, and grown to Day 1 of adulthood. Day 1 worms were heat shocked at 33°C for 1 hour and then recovered for 6 hours at 20°C. Animals were picked free of bacteria and anesthetized with 10 mM levamisole. Worms were mounted onto a 3% agarose pad and imaged using Keyence microscopy. Quantification of GFP intensity was calculated using ImageJ (NIH) by calculating corrected total cell fluorescence (CTCF) for three trials with 20 worms/condition. Significance was determined using the student's t-test (* $p>0.05$).

Thrashing assay

Thrashing/motility was tested by placing 15 Day 1 animals onto a drop of nematode growth media (NGM) buffer on a glass slide and measuring the number of body bends/30 seconds after a 1-minute recovery period. Thrashing data reflects three biologically independent trials. Data was plotted as boxplots using GraphPad Prism (GraphPad Software, https://www.graphpad.com) and was analyzed with a two-tailed *t* test.

Thermotolerance assay

Thermotolerance was tested by exposing Day 1 animals to 37°C heat shock for 3.5 hours and then determining survival 48 hours later by assessing response to a gentle touch. For each trial, ~100 randomly selected individual animals were assessed for the fraction alive (live/total). Thermotolerance assay data reflects three biologically independent trials. Data was plotted as the % survival using GraphPad Prism (GraphPad Software, https://www.graphpad.com) and was analyzed with a two-tailed *t* test.

Statistical analysis

Statistical analyses were carried out with GraphPad Software (GraphPad Software, La Jolla, CA, USA, https://www.graphpad.com) unless otherwise stated. All error bars are representative of standard deviation between independent biological replicates, as indicated.

Results

E3 ligase RNAi does not alter HSP reporter activity after heat stress in wildtype background

Previous studies have found that the levels of HSF-1, the regulator behind the protein quality control machinery, are decreased in Huntington's and Parkinson's disease cell models (Gomez-Pastor et al., 2017; E. Kim et al., 2016). In Huntington's disease, mutant Huntingtin containing a polyglutamine expansion (mHTT) increases expression of FBXW7, an E3 ligase that ubiquitinates HSF1 for degradation (Gomez-Pastor et al., 2017). In Parkinson's disease, the presence of mutant α-synuclein increases expression of E3 ligase NEDD4, which ubiquitinates HSF1 and sends it for proteasomal degradation (E. Kim et al., 2016). Depletion of HSF1 in both diseases leads to an increase in protein aggregation and toxicity (Figure 4.1A). To examine this regulation in *C. elegans,* we utilized RNAi for the respective worm homologs of these E3 ligases, *sel-10* and Y92H12A.2 (Figure 4.1B).

To determine if SEL-10 and Y92H12A.2 regulate the HSR in *C. elegans*, we utilized the HSP transcriptional reporter TJ375. This strain contains a transgene integrated in the genome that utilizes the *hsp-16.2* promoter to drive the expression of GFP to allow for fluorescent quantification of *hsp-16.2* activity after heat shock. We induced RNAi for EV control, *sel-10* RNAi, and Y92H12A.2 RNAi 19 hours after the L1 stage until Day 1 of adulthood, when we heat shocked the worms for 1 hour at 33°C and subsequently allowed recovery for 6 hours. We

measured GFP fluorescence of non-heat shocked and heat shocked worms. We found that compared to control, SEL-10 and Y92H12A.2 did not significantly alter *hsp-16.2* reporter activity in the wildtype background (Figure 4.2).

Similarly, we also used the HSP transcriptional report AM446, which utilizes the *hsp-70* promoter to drive GFP expression. We quantified GFP fluorescence before and after heat shock with *sel-10* and Y92H12A.2 RNAi using the same conditions. We also found that *sel-10* and Y92H12A.2 knockdown did not significantly change *hsp-70* reporter activity in the wildtype background (Figure 4.3). Overall, E3 ligase RNAi did not affect HSP reporter activity in the wildtype background.

E3 ligase RNAi enhances motility in polyQ Huntington's disease model

We next wanted to examine SEL-10 and Y92H12A.2 regulation in a neurodegenerative disease background to determine if the presence of the protein aggregate toxicity of the disease model attributes to the regulation of the HSR. We utilized a Huntington's disease model, AM140, that expresses one polyglutamine (polyQ) expansion of 35 glutamine residues of the Huntingtin protein using a muscle-specific promoter tagged with YFP (Q35::YFP) (Cornaglia et al., 2016). These Q35::YFP worms transition from soluble polyglutamine expression to aggregating polyglutamine expression with age (Cornaglia et al., 2016). We examined motility in aged worms on Day 3 of adulthood where polyQ aggregates have formed. We found that RNAi of *sel-10* and Y92H12A.2 significantly increased motility in the Huntington's disease background (Figure 4.4).

E3 ligase RNAi increases thermotolerance in polyQ Huntington's disease model

We then wanted to test whether CBP-1 also regulates other physiological readouts of the HSR. To test for resistance to heat stress, we examined thermotolerance, a physiological effect known to be modulated by HSF-1. To test this, we fed the worms *sel-10*, Y92H12A.2, or control RNAi from 19 hrs after L1 until Day 3 of adulthood prior to subjecting the worms to a lethal heat shock of 37ºC for 3.5 hours. After a 48-hour recovery, the worms were scored alive/dead after a gentle touch. We examined thermotolerance in the N2 wildtype background and in the Huntington's disease model background. In wildtype worms, compared to empty vector control RNAi-treated worms, *sel-10* and Y92H12A.2 RNAi worms had similar % survival after heat (Figure 4.5). However, in the Huntington's disease model, *sel-10* and Y92H12A.2 RNAi worms has significantly increased survival compared to control worms (Figure 4.5). Thus, only in the Huntington's disease background was there and increase in survivability after severe heat stress under E3 ligase knockdown.

Discussion

Given the importance of HSF-1 degradation in neurodegenerative disease, we sought to elucidate the effect of E3 ligase regulation on the HSR. Here, we examined HSP reporter activity under E3 ligase knockdown and found that SEL-10 and Y92H12A.2 did not alter HSP activity in the wildtype background. In addition, we examined E3 ligase knockdown in a Huntington's disease background and found that *sel-10* and Y92H12A.2 RNAi increased motility and thermotolerance. Overall, these studies suggest a role for SEL-10 and Y92H12A.2 in negatively regulating HSF-1 activity specifically in the Huntington's disease background.

Our data suggests that the E3 ligases SEL-10 and Y92H12A.2 negatively regulate the HSR only in the presences of Huntington's disease polyglutamine protein aggregates. However, further work is needed to elucidate the full scope of their regulation. It is unclear if either E3 ligase directly ubiquitinates HSF-1, leading to its degradation. Are these E3 ligases directly regulating HSF-1 through ubiquitination or through an axillary mechanism? Similarly, can we see a similar negative regulation in other neurodegenerative disease backgrounds? Uncovering these answers will give a better understanding of if the HSF-1 degradation mechanism of neurodegenerative diseases is conserved in *C. elegans*. Further studies are needed to examine overall E3 ligase regulation of HSF-1 and the HSR in *C. elegans*.

A

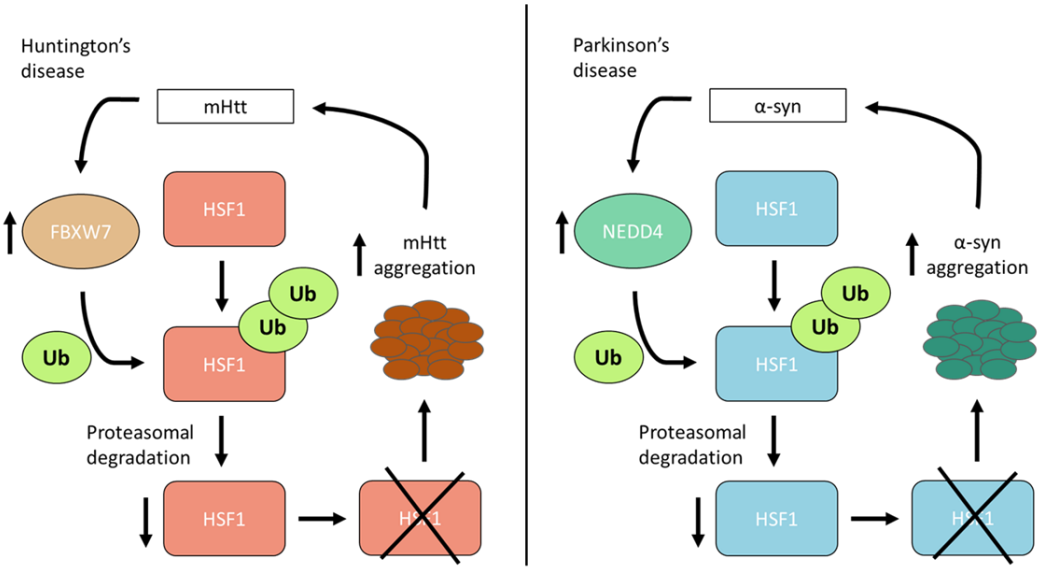

B

Human gene	*C. elegans homolog*
FBXW7	*sel-10*
NEDD4	*Y92H12A.2 (Y92)*

Figure 4.1: Overview of HSF-1 depletion in neurodegenerative disease. A) In healthy cells, the heat shock response activates when under proteotoxic stress via activation of heat shock transcription factor 1 (HSF1). In Huntington's disease, mutant Huntingtin containing a polyglutamine expansion (mHTT) increases expression of FBXW7, an E3 ligase that ubiquitinates HSF1 for degradation (Gomez-Pastor et al., 2017). In Parkinson's disease, the presence of mutant α-synuclein increases expression of E3 ligase NEDD4, which ubiquitinates HSF1 and sends it for proteasomal degradation (E. Kim et al., 2016). Depletion of HSF1 in both diseases leads to an increase in protein aggregation and toxicity. **B)** List of E3 ligases known to ubiquitinate HSF1 and their *C. elegans* homologs.

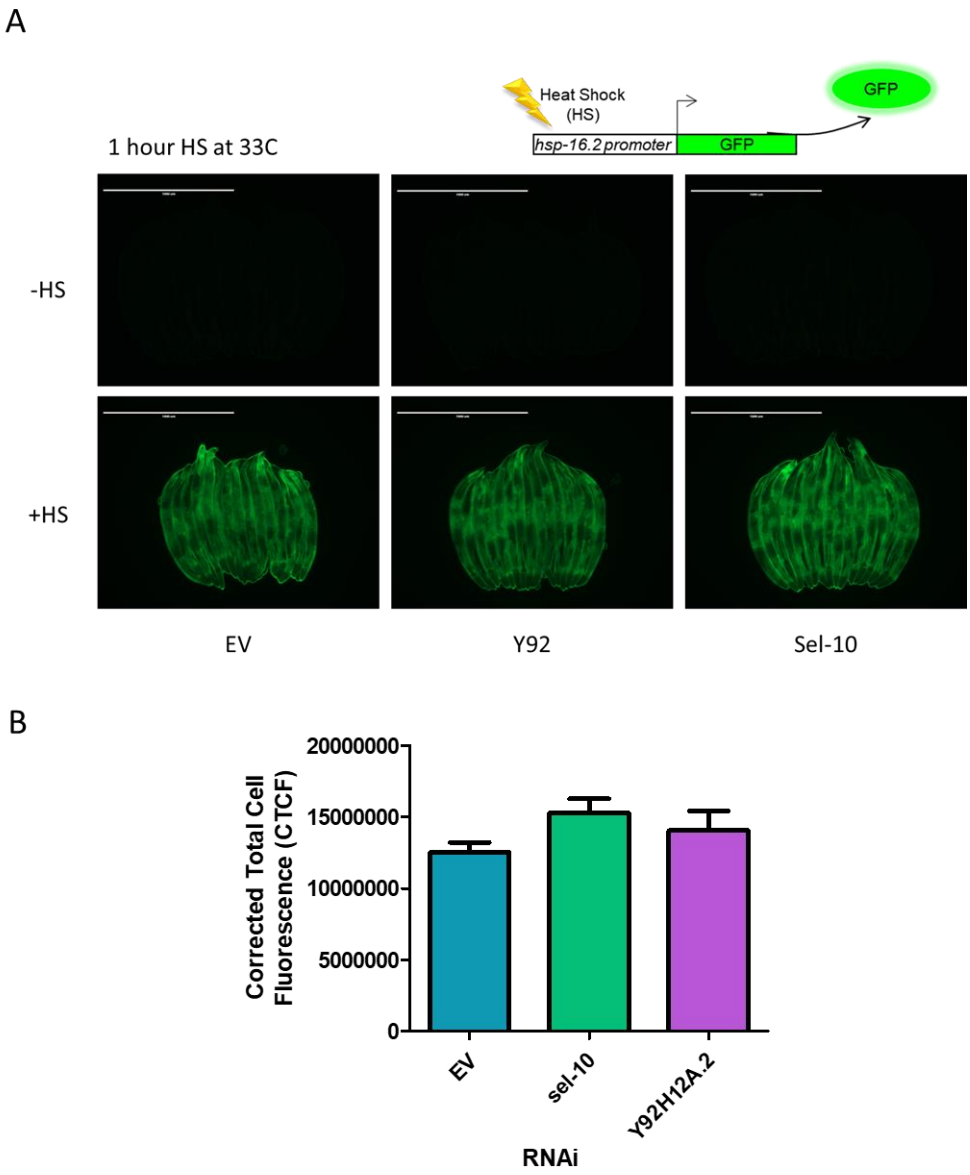

Figure 4.2: E3 ligase RNAi does not alter *hsp-16.2* reporter activity after heat stress in wildtype background. TJ375 (p*hsp-16.2*::GFP) worms were grown on EV, *sel-10*, or Y92H12A.2 RNAi until Day 1 of adulthood. Worms were then exposed to a 1-hour heat shock at 33°C and then recovered for 6 hours at 20°C. Approximately 20 worms were anesthetized with 10mM levamisole and imaged using fluorescent microscopy. GFP fluorescence was quantified using ImageJ (NIH). Experiment was conducted in biological triplicate and statistics were analyzed using GraphPad Prism (GraphPad Software, www.graphpad.com) and was analysed with a two-tailed t test. *p-value < 0.05.

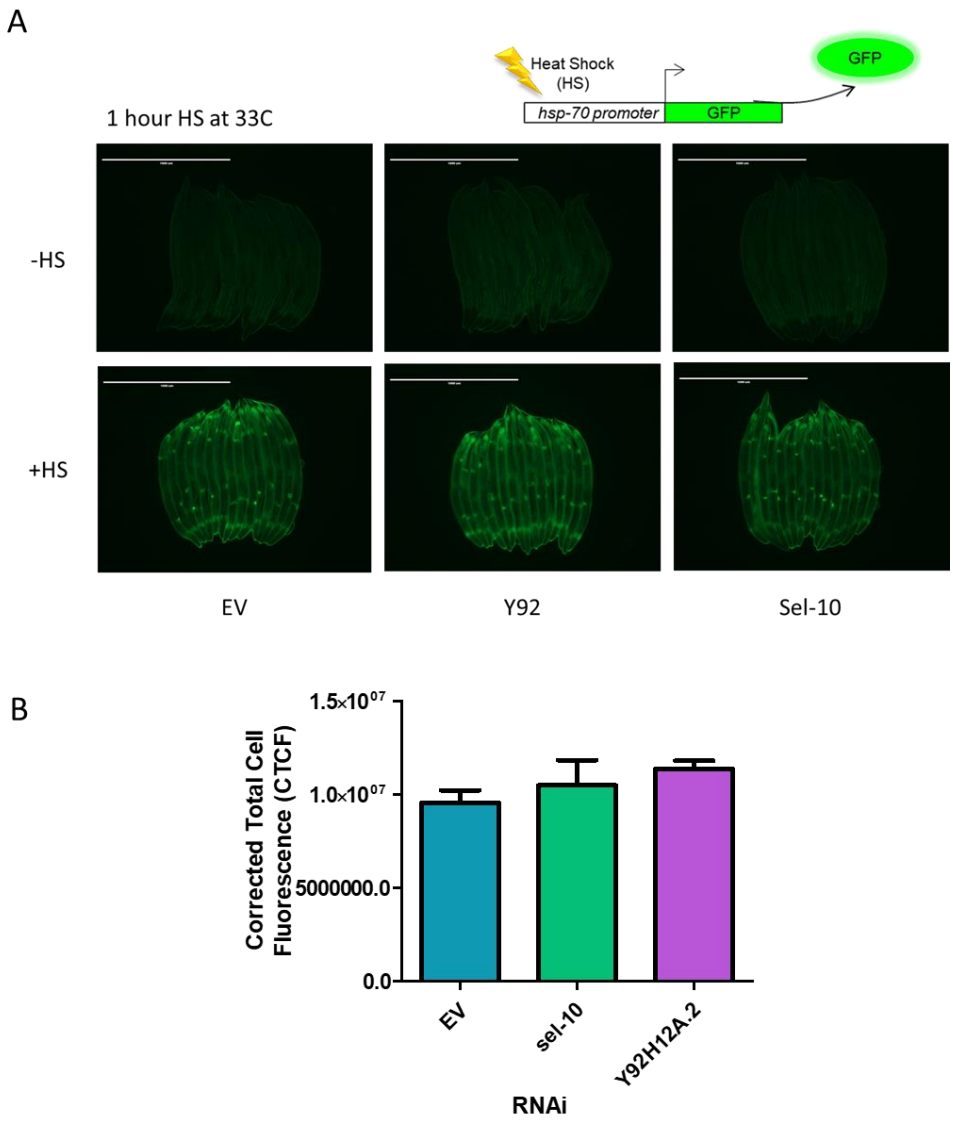

Figure 4.3: E3 ligase RNAi does not alter *hsp-70* reporter activity after heat stress in wildtype background. AM446 (p*hsp-70*::GFP) worms were grown on EV, *sel-10*, or Y92H12A.2 RNAi until Day 1 of adulthood. Worms were then exposed to a 1-hour heat shock at 33°C and then recovered for 6 hours at 20°C. Approximately 20 worms were anesthetized with 10mM levamisole and imaged using fluorescent microscopy. GFP fluorescence was quantified using ImageJ (NIH). Experiment was conducted in biological triplicate and statistics were analyzed using GraphPad Prism (GraphPad Software, www.graphpad.com) and was analysed with a two-tailed t test. *p-value < 0.05.

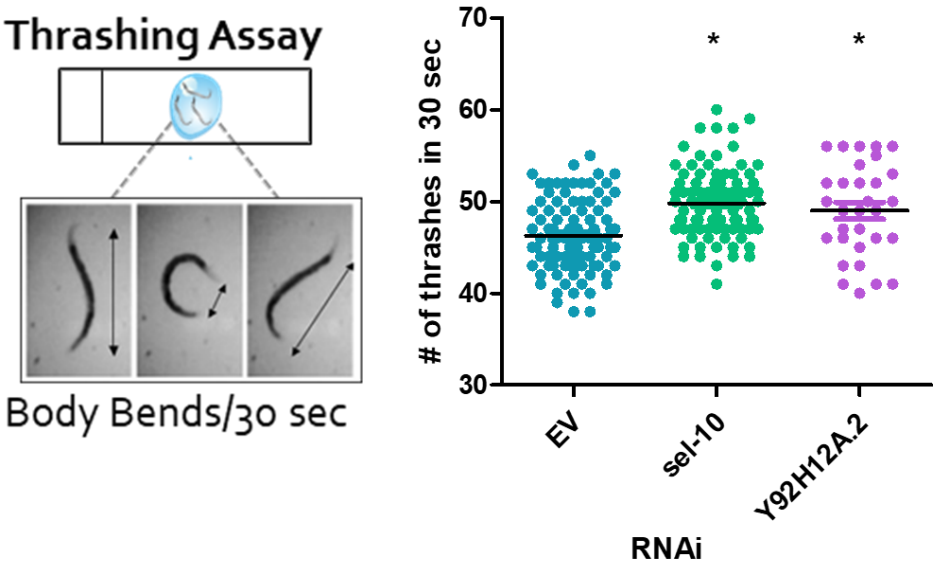

Figure 4.4: E3 ligase RNAi enhances motility in polyQ Huntington's disease model. Motility of the AM140 Huntington's strain under EV, Y92H12A.2 or *sel-10* RNAi was measured by placing Day 3 worms in a drop of NGM buffer and counting the number of thrashes in 30 seconds after a 1-minute recovery period(n=~15 worms). Thrashing assay was conducted in biological triplicate and statistics were analyzed using GraphPad Prism (GraphPad Software, www.graphpad.com) and was analyzed with a two-tailed t test. *p-value < 0.05.

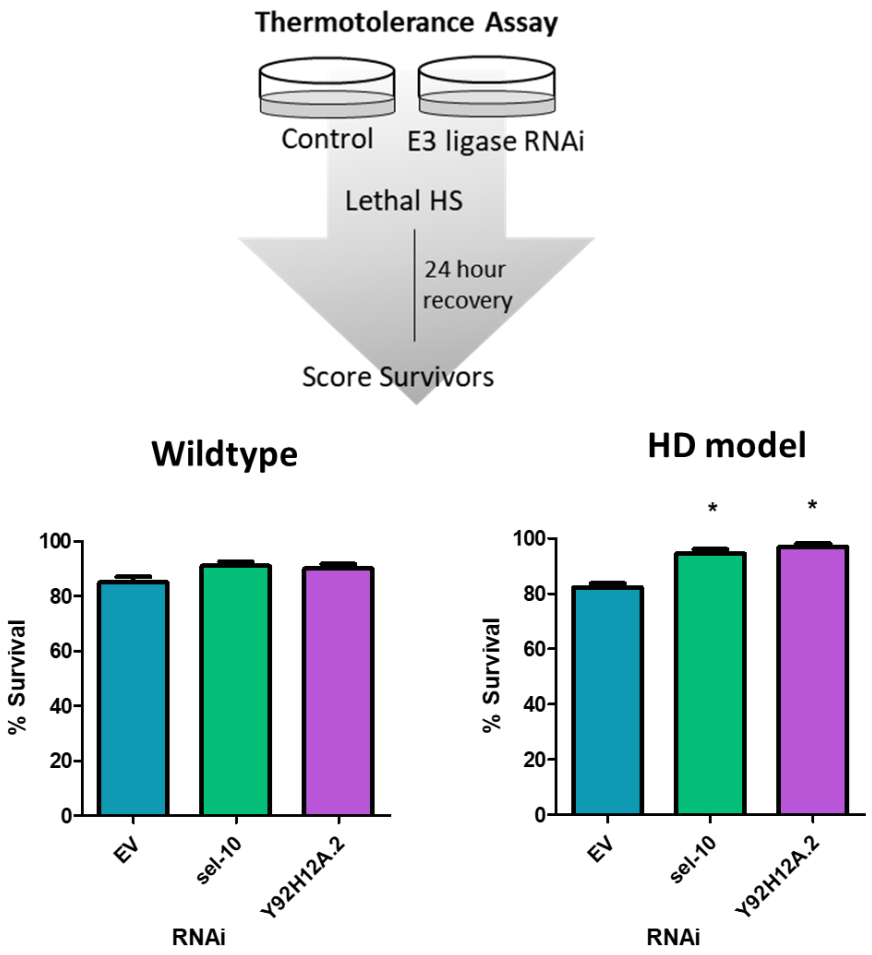

Figure 4.5: E3 ligase RNAi increases thermotolerance in polyQ Huntington's disease model. Thermotolerance of the wildtype (N2) strain and the Huntington's disease (AM140) strain was measured by subjecting the worms to a severe heat shock at 37 ℃ for 2 hours and measuring survival after a 24-hour recovery. Percent survival was determined for worms fed with empty vector (EV), Y92H12A.2, and *sel-10* RNAi. Data was plotted as % survival using GraphPad Prism (GraphPad Software, www.graphpad.com) and was analyzed with a two-tailed t test. *p-value < 0.05.

CHAPTER FIVE: IMPLICATIONS AND FUTURE DIRECTIONS

Implications

CBP-1 regulation of the HSR

Our results indicate that CBP-1 negatively regulates the heat shock response and HSF-1 activity in *C. elegans*. However, there are many unanswered questions about this regulation that remain unresolved. For example, the mechanism behind CBP-1 regulation is far from being elucidated. Does CBP-1 utilize its acetyltransferase activity to directly acetylate HSF-1 or is there an indirect mechanism by which CBP-1 controls HSF-1 activity? It is known that CBP-1 in *C. elegans* regulates other stress response transcription factors, however, it is unclear if CBP-1 acetyltransferase activity is required for this regulation (Ganner et al., 2019; T. Y. Li et al., 2021). Understanding how CBP-1 regulates HSF-1 will give us potential insight into how HSF-1 and other stress response transcription factors may be influenced by lysine acetyltransferases.

Additionally, we found that CBP-1 knockdown increases the recovery rate of nuclear stress bodies. The overall function of nuclear stress bodies is still an outstanding question in the literature. Recent studies suggest the resolution of nSBs correlates with HSF1 activity, transcription of *hsp* target genes, and cell survival at the single cell level (Gaglia et al., 2020). A recent mammalian study discovered the existence of both HSF1 nSBs at non-*hsp* gene loci and smaller HSF1 condensates at transcriptionally active *hsp* gene loci upon heat shock (H. Zhang et al., 2022). How CBP-1 plays a role in the functionality of nuclear stress bodies, not just via HSF-1, could give us insight into the overall function of nuclear stress bodies as a whole. As well, we

examined CBP-1 regulation on nSBs in hypodermal cells, but it may also be important to examine other tissue types. HSF-1 expression and localization is distinct between certain tissue types (Deonarine et al., 2021). Understanding CBP-1 regulation in a tissue-specific manner could reveal more about its function in nuclear stress bodies.

HSR regulation in neurodegenerative disease

Our data suggests that *hsf-1* gene expression is downregulated in the presence of amyloid-beta in an Alzheimer's disease model. Here we utilized whole-worm RNA isolation, but it would be interesting to examine tissue-specific gene expression solely in tissues expressing the protein aggregates examining. Understanding how HSF-1 is affected by the presence of neurodegenerative disease protein aggregates at this level will give a better insight into its regulation of the HSR. Examining HSF-1 regulation at the protein level would also help determine the mechanism of neurodegenerative disease regulation. In mammals, the downregulation of HSF1 in neurodegenerative disease is at the protein level (Gomez-Pastor et al., 2017; E. Kim et al., 2016). Utilizing the created HSF-1::GFPxAβ1-42 strain (SDW068) can provide more insight into this regulation in *C. elegans*.

While we found *hsf-1* gene expression to be downregulated in the Alzheimer's disease model, we found that HSF-1 target genes *hsp-16.2* and *hsp-70* gene expression to be unregulated. This conflict suggests that further research be performed to identify the kinetics of active HSF-1 and if there are potentially other mechanism by which HSPs are being activated. It is possible that other transcription factors can also activate HSPs. It will be insightful to identify if these alternative pathways for HSP induction are being utilized as *hsf-1* gene expression is being suppressed.

HSF-1 degradation in neurodegenerative disease

Our data suggests that the E3 ligases SEL-10 and Y92H12A.2 negatively regulate the HSR only in the presences of Huntington's disease polyglutamine protein aggregates. However, further work is needed to elucidate the full scope of their regulation. It is unclear if either E3 ligase directly ubiquitinates HSF-1, leading to its degradation. Are these E3 ligases directly regulating HSF-1 through ubiquitination or through an axillary mechanism? Similarly, can we see a similar negative regulation in other neurodegenerative disease backgrounds? Uncovering these answers will give a better understanding of if the HSF-1 degradation mechanism of neurodegenerative diseases is conserved in *C. elegans*. With this insight, we can further examine other E3 ligase regulation of HSF-1 and the HSR through the ease of RNAi screening in *C. elegans*.

Future Study 1: Mechanism of CBP-1 regulation of the heat shock response

Identifying the mechanism of CBP-1 regulation on the heat shock response has large appeal. We found that CBP-1 negatively regulates HSP expression, nuclear stress body recovery, and thermotolerance ability of the worm. Thus, future work is needed to determine the precise mechanism of action of CBP-1 in the HSR pathway and any potential acetylation changes of HSF-1 that are induced by CBP-1, given its acetyltransferase function. Specifically, does CBP-1 regulate HSF-1 binding to promotors? Does CBP-1 acetylate HSF-1? To answer these questions, we could utilize our HSF-1::GFP to perform chromatin-immunoprecipitation (Ch-IP) to determine if CBP-1 alters the activation of HSF-1 and its ability to bind to its target promoters after heat stress. Similarly, we could perform co-immunoprecipitation (Co-IP) to pull down HSF-1 and utilize mass spectrometry to identify HSF-1 acetylation changes with and without *cbp-1* RNAi. It would also be interesting to identify HSF-1 binding partners via Co-IP and mass spectrometry. It is unknown if HSF-1 and CBP-1 directly bind. Overall, the mechanism of CBP-

1 regulation on the HSR is not fully elucidated and examining HSF-1 protein levels with CBP-1 would be an interesting future study to uncover CBP-1's mechanism of action in the HSR.

Future Study 2: HSF-1 and nuclear stress body changes in neurodegenerative disease

To visualize HSF-1 protein levels with age in the Alzheimer's disease model, we have genetically crossed the SDW015 strain containing endogenously expressed HSF-1::GFP with the Alzheimer's model, strain CL2006, which expresses a 42-amino acid beta-amyloid peptide using a muscle-specific promoter that forms protein aggregates with age causing paralysis of the worm (Link, 1995) (Figure 3.3). Using this crossed strain, future experiments could be performed to visualize HSF-1 protein levels in the presence of Aβ in a tissue-specific manner. The fluorescently tagged HSF-1 will allow us to visualize changes in HSF-1 levels as the disease protein aggregates with age via fluorescence microscopy. Since the protein aggregates in the Alzheimer's disease model are localized to the muscle cells, one could compare HSF-1 levels in tissues with and without the disease protein aggregates. This would allow visualization of the tissue-specificity of HSR regulation in the Alzheimer's disease model and determination of how Aβ can influence HSF-1 in a tissue-specific manner.

With this HSF-1::GFP strain, we could also examine the formation and resolution of nuclear stress bodies (Deonarine et al., 2021). Nuclear stress body behavior in neurodegenerative disease has not been examined, thus utilizing this crossed strain to examine nSBs in the presence of Aβ would be of interest. Our previous work has uncovered a regulator of nSB resolution, CBP-1. It would be interesting to examine how the disease state can alter this regulation as well.

Future Study 3: Targeted-RNAi screen for E3 ligase regulators of HSF-1

Previously, two E3 ligases, FBXW7 and NEDD4 respectively, were found to play a role in HSF-1 degradation in Huntington's and Parkinson's disease mouse and cell models. FBXW7 was tested due to its connection to HSF-1 in Huntington's polyglutamine expansion brain cells, and NEDD4 was found to be increased in Parkinson's patients previously (Gomez-Pastor et al., 2017; E. Kim et al., 2016). Since both were hand-picked and not the result of a large-scale screen of E3 ligases, we hypothesize that there are other E3 ligases that play a role in the neurodegenerative disease-induced degradation of HSF-1.

To identify these E3 ligases, one could utilize RNAi against the E3 ligases in the *C. elegans* genome (Ohkumo, Masutani, Eki, & Hanaoka, 2008). There are 171 genes in the *C. elegans* genome that encode proteins containing one of the following E3 ligase domains: HECT-domain, U-box domain, monomeric RING finger domain, or multi-subunit complexes that contain a RING finger domain (Fang, Lorick, Jensen, & Weissman, 2003; Medvar, Raghuram, Pisitkun, Sarkar, & Knepper, 2016). FBXW7 and NEDD4 are conserved in the worm and can be included in the RNAi-targeted screen (J. Li et al., 2002; Maeda, Kohara, Yamamoto, & Sugimoto, 2001). We compiled a list of all E3 ligases with their known human homologs (Table B1/2/3/4). We could conduct an RNAi-targeted screen where RNAi is induced at the L4 developmental stage and grow the worms until Day 4 of adulthood in a 96-well plate format (Lehner, Tischler, & Fraser, 2006). We could grow the worms in the RNAi culture until Day 3 of adulthood when the disease protein aggregates usually begin to fully form in the disease model strains (Ohkumo et al., 2008). Once the E3 ligases that degrade HSF-1 are identified, we could visualize changes in protein aggregation upon age with and without RNAi against the ligases. The goal is to evaluate the effects the specific E3 ligases have on the progression of the protein aggregation in the

neurodegenerative disease models. Overall, it would be interesting to identify the full scope of E3 ligase regulation on the HSR and HSF-1 in *C. elegans*.

REFERENCES

Amin, J., Ananthan, J., & Voellmy, R. (1988). Key features of heat shock regulatory elements. *Mol Cell Biol, 8*(9), 3761-3769. doi:10.1128/mcb.8.9.3761-3769.1988

Anckar, J., & Sistonen, L. (2011). Regulation of HSF1 function in the heat stress response: implications in aging and disease. *Annu Rev Biochem, 80*, 1089-1115. doi:10.1146/annurev-biochem-060809-095203

Bharadwaj, S., Ali, A., & Ovsenek, N. (1999). Multiple components of the HSP90 chaperone complex function in regulation of heat shock factor 1 In vivo. *Mol Cell Biol, 19*(12), 8033-8041. doi:10.1128/MCB.19.12.8033

Biamonti, G., & Vourc'h, C. (2010). Nuclear stress bodies. *Cold Spring Harb Perspect Biol, 2*(6), a000695. doi:10.1101/cshperspect.a000695

Brignull, H. R., Morley, J. F., & Morimoto, R. I. (2007). The stress of misfolded proteins: C. elegans models for neurodegenerative disease and aging. *Adv Exp Med Biol, 594*, 167-189. doi:10.1007/978-0-387-39975-1_15

Budzynski, M. A., Puustinen, M. C., Joutsen, J., & Sistonen, L. (2015). Uncoupling Stress-Inducible Phosphorylation of Heat Shock Factor 1 from Its Activation. *Mol Cell Biol, 35*(14), 2530-2540. doi:10.1128/MCB.00816-14

Cai, H., Dhondt, I., Vandemeulebroucke, L., Vlaeminck, C., Rasulova, M., & Braeckman, B. P. (2019). CBP-1 Acts in GABAergic Neurons to Double Life Span in Axenically Cultured Caenorhabditis elegans. *J Gerontol A Biol Sci Med Sci, 74*(8), 1198-1205. doi:10.1093/gerona/glx206

Cheng, H. C., Qi, R. Z., Paudel, H., & Zhu, H. J. (2011). Regulation and function of protein kinases and phosphatases. *Enzyme Res, 2011*, 794089. doi:10.4061/2011/794089

Chu, B., Zhong, R., Soncin, F., Stevenson, M. A., & Calderwood, S. K. (1998). Transcriptional activity of heat shock factor 1 at 37 degrees C is repressed through phosphorylation on two distinct serine residues by glycogen synthase kinase 3 and protein kinases Calpha and Czeta. *J Biol Chem, 273*(29), 18640-18646. doi:10.1074/jbc.273.29.18640

Cornaglia, M., Krishnamani, G., Mouchiroud, L., Sorrentino, V., Lehnert, T., Auwerx, J., & Gijs, M. A. (2016). Automated longitudinal monitoring of in vivo protein aggregation in neurodegenerative disease C. elegans models. *Mol Neurodegener, 11*, 17. doi:10.1186/s13024-016-0083-6

Cotto, J. J., Kline, M., & Morimoto, R. I. (1996). Activation of heat shock factor 1 DNA binding precedes stress-induced serine phosphorylation. Evidence for a multistep pathway of regulation. *J Biol Chem, 271*(7), 3355-3358. doi:10.1074/jbc.271.7.3355

Dai, C., Dai, S., & Cao, J. (2012). Proteotoxic stress of cancer: implication of the heat-shock response in oncogenesis. *J Cell Physiol, 227*(8), 2982-2987. doi:10.1002/jcp.24017

Deonarine, A., Walker, M. W. G., & Westerheide, S. D. (2021). HSF-1 displays nuclear stress body formation in multiple tissues in Caenorhabditis elegans upon stress and following the transition to adulthood. *Cell Stress Chaperones, 26*(2), 417-431. doi:10.1007/s12192-020-01188-9

Dikic, I. (2017). Proteasomal and Autophagic Degradation Systems. *Annu Rev Biochem, 86*, 193-224. doi:10.1146/annurev-biochem-061516-044908

Eastburn, D. J., & Han, M. (2005). A gain-of-function allele of cbp-1, the Caenorhabditis elegans ortholog of the mammalian CBP/p300 gene, causes an increase in histone acetyltransferase activity and antagonism of activated Ras. *Mol Cell Biol, 25*(21), 9427-9434. doi:10.1128/MCB.25.21.9427-9434.2005

Fang, S., Lorick, K. L., Jensen, J. P., & Weissman, A. M. (2003). RING finger ubiquitin protein ligases: implications for tumorigenesis, metastasis and for molecular targets in cancer. *Semin Cancer Biol, 13*(1), 5-14.

Fay, D. (2006). Genetic mapping and manipulation: chapter 1--Introduction and basics. *WormBook*, 1-12. doi:10.1895/wormbook.1.90.1

Gaglia, G., Rashid, R., Yapp, C., Joshi, G. N., Li, C. G., Lindquist, S. L., . . . Santagata, S. (2020). HSF1 phase transition mediates stress adaptation and cell fate decisions. *Nat Cell Biol, 22*(2), 151-158. doi:10.1038/s41556-019-0458-3

Ganner, A., Gerber, J., Ziegler, A. K., Li, Y., Kandzia, J., Matulenski, T., . . . Neumann-Haefelin, E. (2019). CBP-1/p300 acetyltransferase regulates SKN-1/Nrf cellular levels, nuclear localization, and activity in C. elegans. *Exp Gerontol, 126*, 110690. doi:10.1016/j.exger.2019.110690

Garigan, D., Hsu, A. L., Fraser, A. G., Kamath, R. S., Ahringer, J., & Kenyon, C. (2002). Genetic analysis of tissue aging in Caenorhabditis elegans: a role for heat-shock factor and bacterial proliferation. *Genetics, 161*(3), 1101-1112.

Geiger, T., Wehner, A., Schaab, C., Cox, J., & Mann, M. (2012). Comparative proteomic analysis of eleven common cell lines reveals ubiquitous but varying expression of most proteins. *Mol Cell Proteomics, 11*(3), M111 014050. doi:10.1074/mcp.M111.014050

Golden, N. L., Plagens, R. N., Kim Guisbert, K. S., & Guisbert, E. (2020). Standardized Methods for Measuring Induction of the Heat Shock Response in Caenorhabditis elegans. *J Vis Exp*(161). doi:10.3791/61030

Goldenberg, C. J., Luo, Y., Fenna, M., Baler, R., Weinmann, R., & Voellmy, R. (1988). Purified human factor activates heat shock promoter in a HeLa cell-free transcription system. *J Biol Chem, 263*(36), 19734-19739.

Gomez-Pastor, R., Burchfiel, E. T., Neef, D. W., Jaeger, A. M., Cabiscol, E., McKinstry, S. U., . . . Thiele, D. J. (2017). Abnormal degradation of the neuronal stress-protective transcription factor HSF1 in Huntington's disease. *Nat Commun, 8*, 14405. doi:10.1038/ncomms14405

Gomez-Pastor, R., Burchfiel, E. T., & Thiele, D. J. (2018). Regulation of heat shock transcription factors and their roles in physiology and disease. *Nat Rev Mol Cell Biol, 19*(1), 4-19. doi:10.1038/nrm.2017.73

Guettouche, T., Boellmann, F., Lane, W. S., & Voellmy, R. (2005). Analysis of phosphorylation of human heat shock factor 1 in cells experiencing a stress. *BMC Biochem, 6*, 4. doi:10.1186/1471-2091-6-4

Guisbert, E., Czyz, D. M., Richter, K., McMullen, P. D., & Morimoto, R. I. (2013). Identification of a tissue-selective heat shock response regulatory network. *PLoS Genet, 9*(4), e1003466. doi:10.1371/journal.pgen.1003466

Hajdu-Cronin, Y. M., Chen, W. J., & Sternberg, P. W. (2004). The L-type cyclin CYL-1 and the heat-shock-factor HSF-1 are required for heat-shock-induced protein expression in Caenorhabditis elegans. *Genetics, 168*(4), 1937-1949. doi:10.1534/genetics.104.028423

Han, S. K., Lee, D., Lee, H., Kim, D., Son, H. G., Yang, J. S., . . . Kim, S. (2016). OASIS 2: online application for survival analysis 2 with features for the analysis of maximal lifespan and healthspan in aging research. *Oncotarget, 7*(35), 56147-56152. doi:10.18632/oncotarget.11269

Hartl, F. U., Bracher, A., & Hayer-Hartl, M. (2011). Molecular chaperones in protein folding and proteostasis. *Nature, 475*(7356), 324-332. doi:10.1038/nature10317

Havel, L. S., Li, S., & Li, X. J. (2009). Nuclear accumulation of polyglutamine disease proteins and neuropathology. *Mol Brain, 2*, 21. doi:10.1186/1756-6606-2-21

Hendriks, L. E. L., & Dingemans, A. C. (2017). Heat shock protein antagonists in early stage clinical trials for NSCLC. *Expert Opin Investig Drugs, 26*(5), 541-550. doi:10.1080/13543784.2017.1302428

Hentze, N., Le Breton, L., Wiesner, J., Kempf, G., & Mayer, M. P. (2016). Molecular mechanism of thermosensory function of human heat shock transcription factor Hsf1. *Elife, 5*. doi:10.7554/eLife.11576

Hetz, C., Zhang, K., & Kaufman, R. J. (2020). Mechanisms, regulation and functions of the unfolded protein response. *Nat Rev Mol Cell Biol, 21*(8), 421-438. doi:10.1038/s41580-020-0250-z

Hollien, J., & Weissman, J. S. (2006). Decay of endoplasmic reticulum-localized mRNAs during the unfolded protein response. *Science, 313*(5783), 104-107. doi:10.1126/science.1129631

Holmqvist, P. H., & Mannervik, M. (2013). Genomic occupancy of the transcriptional co-activators p300 and CBP. *Transcription, 4*(1), 18-23. doi:10.4161/trns.22601

Hong, Y., Rogers, R., Matunis, M. J., Mayhew, C. N., Goodson, M. L., Park-Sarge, O. K., & Sarge, K. D. (2001). Regulation of heat shock transcription factor 1 by stress-induced SUMO-1 modification. *J Biol Chem, 276*(43), 40263-40267. doi:10.1074/jbc.M104714200

Hsu, A. L., Murphy, C. T., & Kenyon, C. (2003). Regulation of aging and age-related disease by DAF-16 and heat-shock factor. *Science, 300*(5622), 1142-1145. doi:10.1126/science.1083701

Jiang, Y. Q., Wang, X. L., Cao, X. H., Ye, Z. Y., Li, L., & Cai, W. Q. (2013). Increased heat shock transcription factor 1 in the cerebellum reverses the deficiency of Purkinje cells in Alzheimer's disease. *Brain Res, 1519*, 105-111. doi:10.1016/j.brainres.2013.04.059

Jolly, C., Metz, A., Govin, J., Vigneron, M., Turner, B. M., Khochbin, S., & Vourc'h, C. (2004). Stress-induced transcription of satellite III repeats. *J Cell Biol, 164*(1), 25-33. doi:10.1083/jcb.200306104

Jolly, C., Usson, Y., & Morimoto, R. I. (1999). Rapid and reversible relocalization of heat shock factor 1 within seconds to nuclear stress granules. *Proc Natl Acad Sci U S A, 96*(12), 6769-6774. doi:10.1073/pnas.96.12.6769

Joutsen, J., & Sistonen, L. (2019). Tailoring of Proteostasis Networks with Heat Shock Factors. *Cold Spring Harb Perspect Biol, 11*(4). doi:10.1101/cshperspect.a034066

Kamath, R. S., Fraser, A. G., Dong, Y., Poulin, G., Durbin, R., Gotta, M., . . . Ahringer, J. (2003). Systematic functional analysis of the Caenorhabditis elegans genome using RNAi. *Nature, 421*(6920), 231-237. doi:10.1038/nature01278

Kaufman, R. J. (2002). Orchestrating the unfolded protein response in health and disease. *J Clin Invest, 110*(10), 1389-1398. doi:10.1172/JCI16886

Kim, E., Wang, B., Sastry, N., Masliah, E., Nelson, P. T., Cai, H., & Liao, F. F. (2016). NEDD4-mediated HSF1 degradation underlies alpha-synucleinopathy. *Hum Mol Genet, 25*(2), 211-222. doi:10.1093/hmg/ddv445

Kim, Y. E., Hipp, M. S., Bracher, A., Hayer-Hartl, M., & Hartl, F. U. (2013). Molecular chaperone functions in protein folding and proteostasis. *Annu Rev Biochem, 82*, 323-355. doi:10.1146/annurev-biochem-060208-092442

Kourtis, N., Moubarak, R. S., Aranda-Orgilles, B., Lui, K., Aydin, I. T., Trimarchi, T., . . . Aifantis, I. (2015). FBXW7 modulates cellular stress response and metastatic potential through HSF1 post-translational modification. *Nat Cell Biol, 17*(3), 322-332. doi:10.1038/ncb3121

Kourtis, N., Strikoudis, A., & Aifantis, I. (2015). Emerging roles for the FBXW7 ubiquitin ligase in leukemia and beyond. *Curr Opin Cell Biol, 37*, 28-34. doi:10.1016/j.ceb.2015.09.003

Kulak, N. A., Geyer, P. E., & Mann, M. (2017). Loss-less Nano-fractionator for High Sensitivity, High Coverage Proteomics. *Mol Cell Proteomics, 16*(4), 694-705. doi:10.1074/mcp.O116.065136

Kumari, N., Hassan, M. A., Lu, X., Roeder, R. G., & Biswas, D. (2019). AFF1 acetylation by p300 temporally inhibits transcription during genotoxic stress response. *Proc Natl Acad Sci U S A, 116*(44), 22140-22151. doi:10.1073/pnas.1907097116

Labbadia, J., & Morimoto, R. I. (2015). The biology of proteostasis in aging and disease. *Annu Rev Biochem, 84*, 435-464. doi:10.1146/annurev-biochem-060614-033955

Lee, G., Tanaka, M., Park, K., Lee, S. S., Kim, Y. M., Junn, E., . . . Mouradian, M. M. (2004). Casein kinase II-mediated phosphorylation regulates alpha-synuclein/synphilin-1 interaction and inclusion body formation. *J Biol Chem, 279*(8), 6834-6839. doi:10.1074/jbc.M312760200

Lehner, B., Tischler, J., & Fraser, A. G. (2006). RNAi screens in Caenorhabditis elegans in a 96-well liquid format and their application to the systematic identification of genetic interactions. *Nat Protoc, 1*(3), 1617-1620. doi:10.1038/nprot.2006.245

Lewis, M., Helmsing, P. J., & Ashburner, M. (1975). Parallel changes in puffing activity and patterns of protein synthesis in salivary glands of Drosophila. *Proc Natl Acad Sci U S A, 72*(9), 3604-3608. doi:10.1073/pnas.72.9.3604

Li, J., & Le, W. (2013). Modeling neurodegenerative diseases in Caenorhabditis elegans. *Exp Neurol, 250*, 94-103. doi:10.1016/j.expneurol.2013.09.024

Li, J., Pauley, A. M., Myers, R. L., Shuang, R., Brashler, J. R., Yan, R., . . . Gurney, M. E. (2002). SEL-10 interacts with presenilin 1, facilitates its ubiquitination, and alters A-beta peptide production. *J Neurochem, 82*(6), 1540-1548.

Li, T. Y., Sleiman, M. B., Li, H., Gao, A. W., Mottis, A., Bachmann, A. M., . . . Auwerx, J. (2021). The transcriptional coactivator CBP/p300 is an evolutionarily conserved node that promotes longevity in response to mitochondrial stress. *Nat Aging, 1*(2), 165-178. doi:10.1038/s43587-020-00025-z

Link, C. D. (1995). Expression of human beta-amyloid peptide in transgenic Caenorhabditis elegans. *Proc Natl Acad Sci U S A, 92*(20), 9368-9372.

Lopez-Otin, C., Blasco, M. A., Partridge, L., Serrano, M., & Kroemer, G. (2013). The hallmarks of aging. *Cell, 153*(6), 1194-1217. doi:10.1016/j.cell.2013.05.039

Maeda, I., Kohara, Y., Yamamoto, M., & Sugimoto, A. (2001). Large-scale analysis of gene function in Caenorhabditis elegans by high-throughput RNAi. *Curr Biol, 11*(3), 171-176.

Mavroudis, I. A., Fotiou, D. F., Adipepe, L. F., Manani, M. G., Njau, S. D., Psaroulis, D., . . . Baloyannis, S. J. (2010). Morphological changes of the human purkinje cells and deposition of neuritic plaques and neurofibrillary tangles on the cerebellar cortex of Alzheimer's disease. *Am J Alzheimers Dis Other Demen, 25*(7), 585-591. doi:10.1177/1533317510382892

Medvar, B., Raghuram, V., Pisitkun, T., Sarkar, A., & Knepper, M. A. (2016). Comprehensive database of human E3 ubiquitin ligases: application to aquaporin-2 regulation. *Physiol Genomics, 48*(7), 502-512. doi:10.1152/physiolgenomics.00031.2016

Mendillo, M. L., Santagata, S., Koeva, M., Bell, G. W., Hu, R., Tamimi, R. M., . . . Lindquist, S. (2012). HSF1 drives a transcriptional program distinct from heat shock to support highly malignant human cancers. *Cell, 150*(3), 549-562. doi:10.1016/j.cell.2012.06.031

Meng, L., Gabai, V. L., & Sherman, M. Y. (2010). Heat-shock transcription factor HSF1 has a critical role in human epidermal growth factor receptor-2-induced cellular transformation and tumorigenesis. *Oncogene, 29*(37), 5204-5213. doi:10.1038/onc.2010.277

Mercier, P. A., Winegarden, N. A., & Westwood, J. T. (1999). Human heat shock factor 1 is predominantly a nuclear protein before and after heat stress. *J Cell Sci, 112 (Pt 16)*, 2765-2774. doi:10.1242/jcs.112.16.2765

Morley, J. F., & Morimoto, R. I. (2004). Regulation of longevity in Caenorhabditis elegans by heat shock factor and molecular chaperones. *Mol Biol Cell, 15*(2), 657-664. doi:10.1091/mbc.e03-07-0532

Morton, E. A., & Lamitina, T. (2013). Caenorhabditis elegans HSF-1 is an essential nuclear protein that forms stress granule-like structures following heat shock. *Aging Cell, 12*(1), 112-120. doi:10.1111/acel.12024

Mosser, D. D., Theodorakis, N. G., & Morimoto, R. I. (1988). Coordinate changes in heat shock element-binding activity and HSP70 gene transcription rates in human cells. *Mol Cell Biol, 8*(11), 4736-4744. doi:10.1128/mcb.8.11.4736-4744.1988

Muchowski, P. J., & Wacker, J. L. (2005). Modulation of neurodegeneration by molecular chaperones. *Nat Rev Neurosci, 6*(1), 11-22. doi:10.1038/nrn1587

Narita, T., Weinert, B. T., & Choudhary, C. (2019). Functions and mechanisms of non-histone protein acetylation. *Nat Rev Mol Cell Biol, 20*(3), 156-174. doi:10.1038/s41580-018-0081-3

Nasrin, N., Ogg, S., Cahill, C. M., Biggs, W., Nui, S., Dore, J., . . . Alexander-Bridges, M. C. (2000). DAF-16 recruits the CREB-binding protein coactivator complex to the insulin-like growth factor binding protein 1 promoter in HepG2 cells. *Proc Natl Acad Sci U S A, 97*(19), 10412-10417. doi:10.1073/pnas.190326997

Neef, D. W., Jaeger, A. M., & Thiele, D. J. (2011). Heat shock transcription factor 1 as a therapeutic target in neurodegenerative diseases. *Nat Rev Drug Discov, 10*(12), 930-944. doi:10.1038/nrd3453

Nussbaum-Krammer, C. I., & Morimoto, R. I. (2014). Caenorhabditis elegans as a model system for studying non-cell-autonomous mechanisms in protein-misfolding diseases. *Dis Model Mech, 7*(1), 31-39. doi:10.1242/dmm.013011

Ohkumo, T., Masutani, C., Eki, T., & Hanaoka, F. (2008). Use of RNAi in C. elegans. *Methods Mol Biol, 442*, 129-137. doi:10.1007/978-1-59745-191-8_10

Papaevgeniou, N., & Chondrogianni, N. (2014). The ubiquitin proteasome system in Caenorhabditis elegans and its regulation. *Redox Biol, 2*, 333-347. doi:10.1016/j.redox.2014.01.007

Parker, C. S., & Topol, J. (1984). A Drosophila RNA polymerase II transcription factor binds to the regulatory site of an hsp 70 gene. *Cell, 37*(1), 273-283. doi:10.1016/0092-8674(84)90323-4

Pierce, A., Podlutskaya, N., Halloran, J. J., Hussong, S. A., Lin, P. Y., Burbank, R., . . . Galvan, V. (2013). Over-expression of heat shock factor 1 phenocopies the effect of chronic inhibition of TOR by rapamycin and is sufficient to ameliorate Alzheimer's-like deficits in mice modeling the disease. *J Neurochem, 124*(6), 880-893. doi:10.1111/jnc.12080

Raychaudhuri, S., Loew, C., Korner, R., Pinkert, S., Theis, M., Hayer-Hartl, M., . . . Hartl, F. U. (2014). Interplay of acetyltransferase EP300 and the proteasome system in regulating heat shock transcription factor 1. *Cell, 156*(5), 975-985. doi:10.1016/j.cell.2014.01.055

Ritossa, F. (1996). Discovery of the heat shock response. *Cell Stress Chaperones, 1*(2), 97-98. doi:10.1379/1466-1268(1996)001<0097:dothsr>2.3.co;2

Rosenberger, A. F., Morrema, T. H., Gerritsen, W. H., van Haastert, E. S., Snkhchyan, H., Hilhorst, R., . . . Hoozemans, J. J. (2016). Increased occurrence of protein kinase CK2 in astrocytes in Alzheimer's disease pathology. *J Neuroinflammation, 13*, 4. doi:10.1186/s12974-015-0470-x

Sheikh, B. N., & Akhtar, A. (2019). The many lives of KATs - detectors, integrators and modulators of the cellular environment. *Nat Rev Genet, 20*(1), 7-23. doi:10.1038/s41576-018-0072-4

Shi, Y., Kroeger, P. E., & Morimoto, R. I. (1995). The carboxyl-terminal transactivation domain of heat shock factor 1 is negatively regulated and stress responsive. *Mol Cell Biol, 15*(8), 4309-4318. doi:10.1128/MCB.15.8.4309

Shi, Y., & Mello, C. (1998). A CBP/p300 homolog specifies multiple differentiation pathways in Caenorhabditis elegans. *Genes Dev, 12*(7), 943-955. doi:10.1101/gad.12.7.943

Sivery, A., Courtade, E., & Thommen, Q. (2016). A minimal titration model of the mammalian dynamical heat shock response. *Phys Biol, 13*(6), 066008. doi:10.1088/1478-3975/13/6/066008

Sorger, P. K., & Nelson, H. C. (1989). Trimerization of a yeast transcriptional activator via a coiled-coil motif. *Cell, 59*(5), 807-813. doi:10.1016/0092-8674(89)90604-1

Spradling, A., Pardue, M. L., & Penman, S. (1977). Messenger RNA in heat-shocked Drosophila cells. *J Mol Biol, 109*(4), 559-587. doi:10.1016/s0022-2836(77)80091-0

Sullivan, E. K., Weirich, C. S., Guyon, J. R., Sif, S., & Kingston, R. E. (2001). Transcriptional activation domains of human heat shock factor 1 recruit human SWI/SNF. *Mol Cell Biol, 21*(17), 5826-5837. doi:10.1128/MCB.21.17.5826-5837.2001

van Ham, T. J., Thijssen, K. L., Breitling, R., Hofstra, R. M., Plasterk, R. H., & Nollen, E. A. (2008). C. elegans model identifies genetic modifiers of alpha-synuclein inclusion formation during aging. *PLoS Genet, 4*(3), e1000027. doi:10.1371/journal.pgen.1000027

Victor, M., Bei, Y., Gay, F., Calvo, D., Mello, C., & Shi, Y. (2002). HAT activity is essential for CBP-1-dependent transcription and differentiation in Caenorhabditis elegans. *EMBO Rep, 3*(1), 50-55. doi:10.1093/embo-reports/kvf006

Vora, M., Shah, M., Ostafi, S., Onken, B., Xue, J., Ni, J. Z., . . . Driscoll, M. (2013). Deletion of microRNA-80 activates dietary restriction to extend C. elegans healthspan and lifespan. *PLoS Genet, 9*(8), e1003737. doi:10.1371/journal.pgen.1003737

Vuister, G. W., Kim, S. J., Orosz, A., Marquardt, J., Wu, C., & Bax, A. (1994). Solution structure of the DNA-binding domain of Drosophila heat shock transcription factor. *Nat Struct Biol, 1*(9), 605-614.

Wang, Y., & Le, W. D. (2019). Autophagy and Ubiquitin-Proteasome System. *Adv Exp Med Biol, 1206*, 527-550. doi:10.1007/978-981-15-0602-4_25

Westerheide, S. D., Anckar, J., Stevens, S. M., Jr., Sistonen, L., & Morimoto, R. I. (2009). Stress-inducible regulation of heat shock factor 1 by the deacetylase SIRT1. *Science, 323*(5917), 1063-1066. doi:10.1126/science.1165946

Westerheide, S. D., Raynes, R., Powell, C., Xue, B., & Uversky, V. N. (2012). HSF transcription factor family, heat shock response, and protein intrinsic disorder. *Curr Protein Pept Sci, 13*(1), 86-103. doi:10.2174/138920312799277956

Whitesell, L., & Lindquist, S. L. (2005). HSP90 and the chaperoning of cancer. *Nat Rev Cancer, 5*(10), 761-772. doi:10.1038/nrc1716

Wiederrecht, G., Shuey, D. J., Kibbe, W. A., & Parker, C. S. (1987). The Saccharomyces and Drosophila heat shock transcription factors are identical in size and DNA binding properties. *Cell, 48*(3), 507-515. doi:10.1016/0092-8674(87)90201-7

Wu, B. J., Kingston, R. E., & Morimoto, R. I. (1986). Human HSP70 promoter contains at least two distinct regulatory domains. *Proc Natl Acad Sci U S A, 83*(3), 629-633. doi:10.1073/pnas.83.3.629

Wu, J., Rutkowski, D. T., Dubois, M., Swathirajan, J., Saunders, T., Wang, J., . . . Kaufman, R. J. (2007). ATF6alpha optimizes long-term endoplasmic reticulum function to protect cells from chronic stress. *Dev Cell, 13*(3), 351-364. doi:10.1016/j.devcel.2007.07.005

Yang, Y., He, Y., Wang, X., Liang, Z., He, G., Zhang, P., . . . Liang, S. (2017). Protein SUMOylation modification and its associations with disease. *Open Biol, 7*(10). doi:10.1098/rsob.170167

Zelin, E., & Freeman, B. C. (2015). Lysine deacetylases regulate the heat shock response including the age-associated impairment of HSF1. *J Mol Biol, 427*(7), 1644-1654. doi:10.1016/j.jmb.2015.02.010

Zhang, H., Shao, S., Zeng, Y., Wang, X., Qin, Y., Ren, Q., . . . Sun, Y. (2022). Reversible phase separation of HSF1 is required for an acute transcriptional response during heat shock. *Nat Cell Biol, 24*(3), 340-352. doi:10.1038/s41556-022-00846-7

Zhang, M., Poplawski, M., Yen, K., Cheng, H., Bloss, E., Zhu, X., . . . Mobbs, C. V. (2009). Role of CBP and SATB-1 in aging, dietary restriction, and insulin-like signaling. *PLoS Biol, 7*(11), e1000245. doi:10.1371/journal.pbio.1000245

Zhou, J. B., Zheng, Y. L., Zeng, Y. X., Wang, J. W., Pei, Z., & Pang, J. Y. (2018). Marine derived xyloketal derivatives exhibit anti-stress and anti-ageing effects through HSF pathway in Caenorhabditis elegans. *Eur J Med Chem, 148*, 63-72. doi:10.1016/j.ejmech.2018.02.028

Zhou, L., He, B., Deng, J., Pang, S., & Tang, H. (2019). Histone acetylation promotes long-lasting defense responses and longevity following early life heat stress. *PLoS Genet, 15*(4), e1008122. doi:10.1371/journal.pgen.1008122

Zou, J., Guo, Y., Guettouche, T., Smith, D. F., & Voellmy, R. (1998). Repression of heat shock transcription factor HSF1 activation by HSP90 (HSP90 complex) that forms a stress-sensitive complex with HSF1. *Cell, 94*(4), 471-480. doi:10.1016/s0092-8674(00)81588-3

APPENDIX A: SUPPLEMENTAL FIGURES FOR CHAPTER TWO

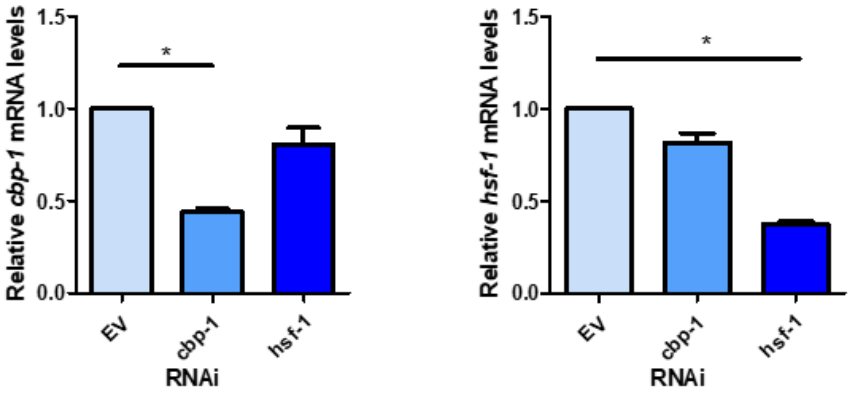

Figure A1: Validation of *hsf-1* RNAi. RNA was extracted from wildtype (N2) worms on Day 1 of adulthood that were fed empty vector (EV), *cbp-1*, or *hsf-1* RNAi beginning 19 hrs after L1. *cbp-1* and *hsf-1* levels were quantified by qRT-PCR (n = 3 biologically independent samples). Statistical analysis determined by determined by conducting a One-Way ANOVA using GraphPad Prism (GraphPad Software, www.graphpad.com) followed by a Tukey post hoc test comparison of all columns. *p-value < 0.05, **p-value < 0.01, ***p-value < 0.001.

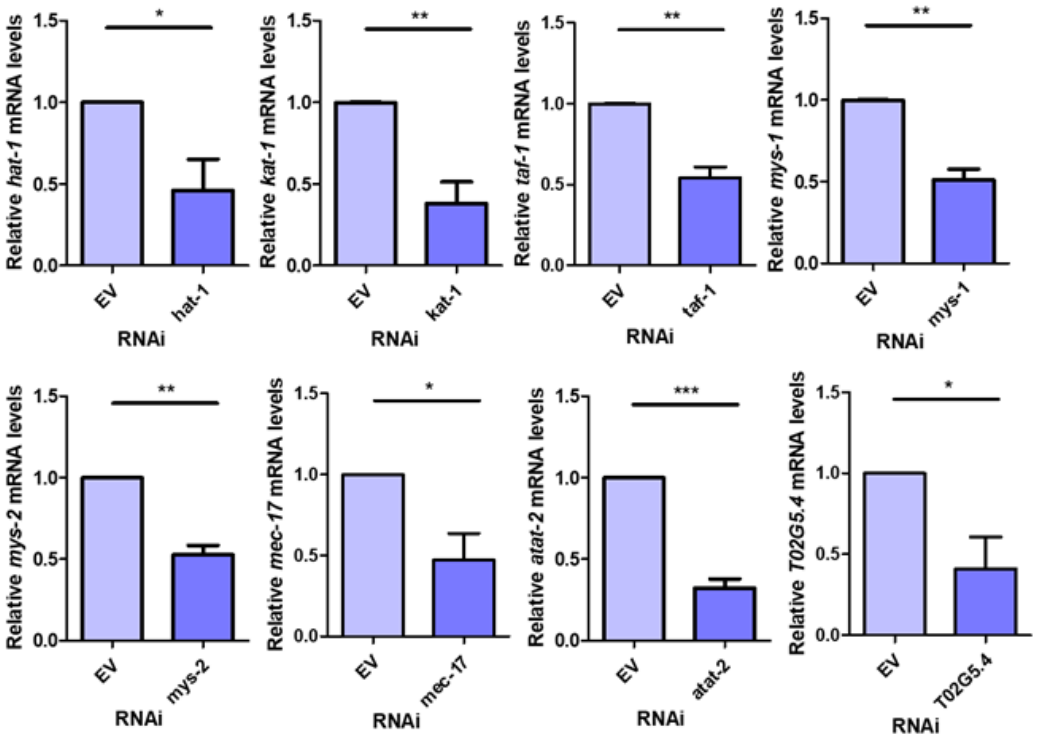

Figure A2: Validation of KAT RNAi. RNA was extracted from N2 worms on Day 1 of adulthood that were fed EV or KAT RNAi beginning 19 hrs after L1. Validation of KAT knockdown was examined by quantifying KAT levels by qRT-PCR (n = 3 biologically independent samples). Statistical analysis determined by determined by conducting a One-Way ANOVA using GraphPad Prism (GraphPad Software, www.graphpad.com) followed by a Tukey post hoc test comparison of all columns. *p-value < 0.05, **p-value < 0.01, ***p-value < 0.001.

A

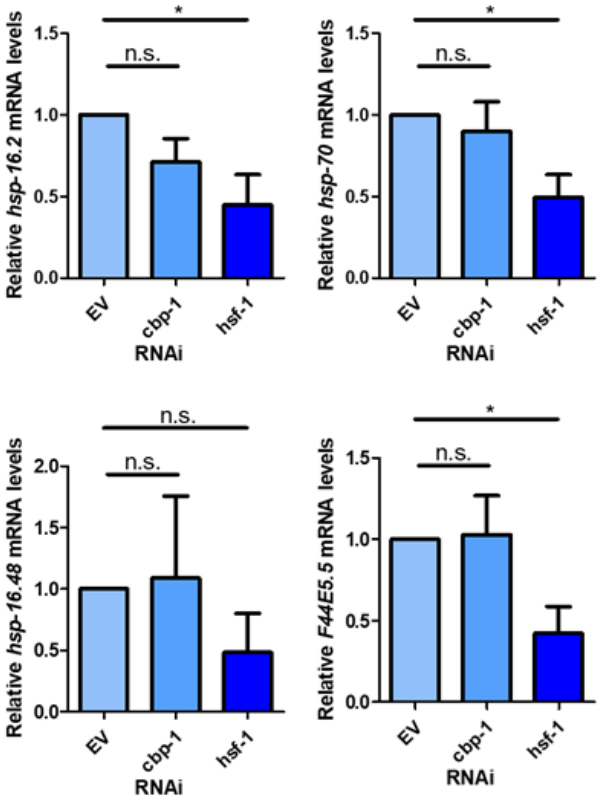

B

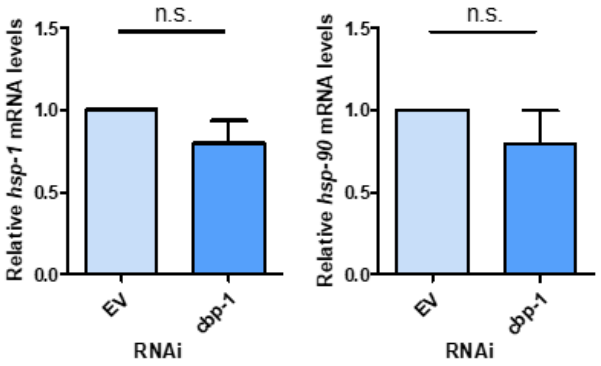

Figure A3: *cbp-1* RNAi does not change the expression of HSF-1 target genes under basal conditions. A) RNA was extracted from N2 (wildtype) worms on Day 1 of adulthood under basal conditions at 20°C that were fed empty vector (EV), *cbp-1*, or *hsf-1* RNAi beginning 19 hrs after L1. Heat shock inducible heat shock protein gene expression levels for *hsp-16.2*, *hsp-16.48*, F44E5.5, and *hsp-70* were quantified by qRT-PCR. **B)** RNA was extracted from N2 worms on Day 1 of adulthood under basal conditions that were fed EV or *cbp-1* RNAi beginning 19 hrs after L1. Developmental HSF-1 target genes independent of the heat shock response, *hsp-1* and *hsp-90*, were quantified by qRT-PCR. Statistical analysis was determined by determined by conducting a One-Way ANOVA using GraphPad Prism (GraphPad Software, www.graphpad.com) followed by a Tukey post hoc test comparison of all columns. *p-value < 0.05.

Table A1: Lifespan analysis of *cbp-1* RNAi. Analysis of lifespan of EV, *cbp-1*, *hsf-1*, and *cbp-1/hsf-1* RNAi including mean lifespan and total/censored/scored number of worms per trial (done in biological triplicate). Survivability was plotted using OASIS 2 (https://sbi.postech.ac.kr/oasis2/) (Han et al. 2016), and statistical analysis was done by Log-rank (Mantel-Cox) Test.

Exp #	RNAi	# animals	# censored	Restricted Mean	
				Days	S.E.
1	EV	110	7	16.49	0.59
2	EV	74	4	16.05	0.7
3	EV	63	5	16.44	0.71
1	cbp-1	79	24	8.79	0.28
2	cbp-1	253	4	9.06	0.11
3	cbp-1	126	8	9.98	0.24
1	hsf-1	218	20	8.19	0.13
2	hsf-1	93	18	8.58	0.21
3	hsf-1	76	2	10.32	0.19
1	cbp-1/hsf-1	163	20	8.38	0.13
2	cbp-1/hsf-1	107	3	8.96	0.17
3	cbp-1/hsf-1	109	5	9.48	0.14

Condition	chi	P-value	Bonferroni P-value
WT v.s. cbp-1	329	0.0000	0.0000
WT v.s. hsf-1	346	0.0000	0.0000
WT v.s. cbp-1/hsf-1	346	0.0000	0.0000
cbp-1 v.s. WT	329	0.0000	0.0000
cbp-1 v.s. hsf-1	12	0.0005	0.0015
cbp-1 v.s. cbp-1/hsf-1	11	0.0008	0.0025
hsf-1 v.s. cbp-1/hsf-1	0	0.7579	1.0000

APPENDIX B: SUPPLEMENTAL TABLES FOR CHAPTER FIVE

Table B1: List of HECT domain E3 ligases in *C. elegans*

Sequence	*C. elegans* E3 ligase	Human Homolog
Hect domain E3s		
C34D4.14	hecd-1	HECTD1 (HECT domain E3 ubiquitin protein ligase 1)
D2085.4	etc-1	UBE3C
F36A2.13	ubr-5	UBR5 (ubiquitin protein ligase E3 component n-recognin 5)
F45H7.6	hecw-1	HECW1 and HECW2 (HECT, C2 and WW domain containing E3 ubiquitin protein ligase 1)
Y39A1C.2	oxi-1	UBE3B
Y48G8AL.1	herc-1	HERC3, HERC4, and HERC6
Y65B4BR.4	wwp-1	ITCH (itchy E3 ubiquitin protein ligase), WWP1 (WW domain containing E3 ubiquitin protein ligase 1)
Y67D8C.5	eel-1	HUWE1 (HECT, UBA and WWE domain containing 1, E3 ubiquitin protein ligase)
Y92H12A.2	-	NEDD4L (neural precursor cell expressed, developmentally down-regulated 4-like, E3 ubiquitin protein ligase) and NEDD4

Table B2: List of Cullin-based E3 ligases in *C. elegans*

Sequence	*C. elegans* E3 ligase	Human Homolog
Cullin-based E3s		
D2045.6	cul-1	CUL1
ZK520.4	cul-2	CUL2
Y108G3AL.1	cul-3	CUL3
F45E12.3	cul-4	CUL4
ZK856.1	cul-5	CUL5
K08E7.7	cul-6	CUL1
K10B2.1	lin-23	BTRC (beta-transducin repeat containing E3 ubiquitin protein ligase) and FBXW11 (F-box and WD repeat domain containing 11)
F55B12.3	sel-10	FBXW7 (F-box and WD repeat domain containing 7)
C26E6.5	fsn-1	FBXO45 (F-box protein 45)

Table B3: List of U-box E3 ligases in *C. elegans*

Sequence	*C. elegans* E3 ligase	Human Homolog
U-box E3s		
F59E10.2		PPIL2
T05H10.5	ufd-2	UBE4B
T09B4.10	chn-1	STUB1
T10F2.4	prp-19	PRPF19 (pre-mRNA processing factor 19)

Table B4: List of monomeric ring finger E3 ligases in *C. elegans*

Sequence	*C. elegans* E3 ligase	Human Homolog
Monomeric Ring Finger E3s		
B0281.3	-	
B0281.8	-	
B0393.6	-	
B0416.4	-	
B0432.13	-	TRAIP
C01B7.6	rpm-1, rpm-3, sam-1, sad-3, syd-3	MYCBP2
C01G6.4	-	RNF11
C02B8.6	-	
C06A5.8	-	
C06A5.9	rnf-1, tag-54	
C09E7.5	-	
C09E7.8	-	
C09E7.9	-	
C11H1.3	-	MGRN1, RNF157
C12C8.3	lin-41	TRIM71
C15F1.5	-	
C16C10.5	rnf-121	RNF121, RNF175
C16C10.7	rnf-5	RNF185
C17E4.3	marc-3	MARCH2, MARCH3
C17H11.6	-	RNF19A, RNF19B
C18B12.4	-	RNF13, RNF167, ZNRF4
C18H9.7	rpy-1, rap-1	RAPSN
C26B9.6	-	
C28G1.5	-	
C28G1.6	-	
C30F2.2	-	
C32D5.10	-	
C32D5.11	-	
C32E8.1	-	
C34E10.4	prx-10, wrs-2, wars-2	WARS2
C34F11.1	-	
C36A4.8	brc-1	Brca1
C36B1.9	-	
C39F7.2	madd-2	
C45G7.4	-	
C49H3.5	ntl-4	CNOT4
C52E12.1	-	
C53A5.6	-	

Table B4 (cont.)

Sequence	*C. elegans* E3 ligase	Human Homolog
Monomeric Ring Finger E3s		
C53D5.2	marc-4	
C55A6.1	-	RNF146
C56A3.4	-	
D2089.2	marc-2	MARCH2
EEED8.16	brap-2	BRAP
F08B12.2	prx-12	PEX12
F08G12.5	-	
F10D7.5	-	NEURL1, NEURL1B
F10G7.10	-	UBR3
F11A10.3	mig-32	PCGF3
F16A11.1	-	RSPRY1
F19G12.1	-	
F23B2.10	-	
F26E4.11	hrdl-1	AMFR (autocrine motility factor receptor)
F26F4.7	nhl-2	
F26G5.9	tam-1	
F32A6.3	vps-41	VPS41
F35G12.9	apc-11	ANAPC11 (anaphase promoting complex subunit 11)
F36F2.3	rbpl-1	RBBP6 (RB binding protein 6, ubiquitin ligase)
F40G9.12	-	
F40G9.14	-	
F42C5.4	-	
F42G2.5	-	VAPA, VAPB
F43C11.7	-	
F43C11.8	-	
F43G6.8	-	
F44D12.10	-	
F45G2.6	trf-1	TRAF4 (TNF receptor associated factor 4)
F46F2.1	-	
F47G9.4	-	RNF207 (ring finger protein 207)
F53F8.3	-	
F53G2.7	mnat-1	MNAT1 (MNAT1, CDK activating kinase assembly factor)
F54B11.5	-	RNF141 (ring finger protein 141)
F54G8.4	nhl-1	TRIM2 (tripartite motif containing 2), TRIM3 (tripartite motif containing 3)
F55A3.1	marc-6	MARCH6 (membrane associated ring-CH-type finger 6)
F55A11.3	sel-11	SYVN1 (synoviolin 1)
F55A11.7	-	

Table B4 (cont.)

Sequence	*C. elegans* E3 ligase	Human Homolog
Monomeric Ring Finger E3s		
F56D2.2	-	RNF14 (ring finger protein 14)
F58B6.3	par-2	
F58E6.1	sta-2	
H05L14.2	-	
H10E21.5	-	RNF148 (ring finger protein 148), RNF149, and RNF150
K01G5.1	rnf-113	RNF113A (ring finger protein 113A) and RNF113B (ring finger protein 113B)
K02B12.8	zhp-3	RNF212B (ring finger protein 212B)
K04C2.4	brd-1	
K09F6.7	-	
K11D12.9	-	
K12B6.8	-	
M02A10.3	sli-1	CBL (Cbl proto-oncogene), CBLB (Cbl proto-oncogene B), and CBLC (Cbl proto-oncogene C)
M88.3	-	
M110.3	-	
M142.6	rle-1	RC3H1 (ring finger and CCCH-type domains 1) and RC3H2 (ring finger and CCCH-type domains 2)
R02E12.4	-	TEKT4 (tektin 4)
R05D3.4	rfp-1	RNF20 (ring finger protein 20) and RNF40 (ring finger protein 40)
R06F6.2	vps-11	VPS11 (VPS11, CORVET/HOPS core subunit)
R10A10.2	rbx-2	RNF7 (ring finger protein 7)
T01C3.3	-	
T01G5.7	-	
T02C1.1	-	
T02C1.2	-	
T05A12.4	-	SHPRH (SNF2 histone linker PHD RING helicase)
T08D2.4	-	
T13A10.2	-	
T13H2.5	spat-3	
T20F5.6	-	
T20F5.7	-	
T22B2.1	-	
T23F6.3	-	
T24D1.2	-	
T24D1.3	-	
T24D1.5	har-2	

Table B4 (cont.)

Sequence	*C. elegans* E3 ligase	Human Homolog
Monomeric Ring Finger E3s		
T26C12.3	-	
W02A11.3	toe-4	RNF111 (ring finger protein 111)
W04H10.3	nhl-3	
W09G3.6	-	
Y4C6A.3	-	
Y6D1A.2	-	
Y7A9C.1	-	
Y38C1AA.6	-	
Y38F1A.2	-	RNF170 (ring finger protein 170)
Y38H8A.2	-	
Y45F10B.8	-	
Y45F10B.9	-	
Y45G12B.2	-	ZFPL1
Y47D3A.22	mib-1	MIB1 (mindbomb E3 ubiquitin protein ligase 1)
Y47D3B.11	plr-1	
Y47G6A.14	-	
Y51F10.2	-	
Y52E8A.2	-	
Y53G8AM.4	-	
Y54E10A.11	-	LTN1 (listerin E3 ubiquitin protein ligase 1)
Y54E10BR.3	-	RNF115 (ring finger protein 115) and RNF126
Y55F3AM.6	lep-2	
Y57A10B.1	marc-5	
Y67D8B.1	-	
Y71F9AL.10	-	ZNRF1 (zinc and ring finger 1)
Y73C8C.7	sdz-34	
Y73C8C.8	-	
Y75B8A.10	-	
Y105C5B.11	-	
Y105E8A.14	-	RNF146 (ring finger protein 146)
Y119C1B.5	rnf-145	RNF145 (ring finger protein 145)
ZC13.1	-	RNFT1 (ring finger protein, transmembrane 1) and RNFT2 (ring finger protein, transmembrane 2)
ZK287.5	rbx-1	RBX1 (ring-box 1)
ZK637.14	-	
ZK809.7	prx-2	
ZK993.2	-	
ZK1240.1	-	

Table B4 (cont.)

Sequence	*C. elegans* E3 ligase	Human Homolog
Monomeric Ring Finger E3s		
ZK1240.2	-	
ZK1240.3	-	
ZK1240.6	-	
ZK1240.8	-	
ZK1240.9	-	
ZK1320.6	arc-1, arl-4	TRIM23 (tripartite motif containing 23)

APPENDIX C: EXTENDED PROTOCOLS

Bleach Synchronization

1. Prep: One 15ml tube and 2 transfer pipets per strain
2. Examine plate for high percentage of gravid adults. If there are no eggs or bacteria on the plate, it is probably starved and should not be used for your experiment.
3. Take out clean NGM plate to warm to room temperature.
4. Wash plate with NGM buffer, use a transfer pipet to pipet worms into a 15 mL tube, repeat plate wash until most of the worms have been removed.
5. Cap tightly, invert 3-4 times, and centrifuge at 1600 rpm for 30 seconds (or allow to sit undisturbed in rack for ~5-7 minutes to gravity settle out the adults).
6. Discard supernatant which contains excess bacteria + larval worms.
7. Wash adults with up to 10 mL of H20 and centrifuge at 1600 rpm for 30 seconds (or allow them to gravity settle again for ~5-7 minutes). You should have a clear supernatant now. If not, rewash with H20 until clean.
8. Remove supernatant to 3.5 mL. Discard transfer pipet.

The rest of the procedure must be done to completion. Take a break now if needed.

9. Quickly add 1000 µL of bleach then 250 µL of NaOH to worms. Cap tube tightly, and continuously and vigorously shake for a maximum of 5 minutes. Worms will typically by lysed around 3-4 minutes.

10. Examine tube for unlysed worm bodies, if you observe no bodies prior to 5 minutes move on to the next step, but no matter what do not lyse for longer than 5 minutes or eggs will begin to be destroyed.
11. After the 5 min bleach, add H20 up to 10 mL and centrifuge tube at 1600 rpm for 30 seconds. Carefully pipet out supernatant using the second transfer pipet, not to disturb the egg pellet.
12. Pour up to 5 mL of H20 to the tube. This should resuspend the eggs into the solution. Centrifuge at 1600 rpm for 30 seconds and remove the supernatant.
13. Repeat step 11 once more to ensure you have removed all the bleach. Leave ~0.5ml of supernatant in the tube.
14. Use the transfer pipet to break up egg clumps (blow bubbles and gently pipet up and down a few times) and resuspend the eggs, then transfer the eggs to a clean NGM plate.
15. Observe plate for clean vs. messy bleach (only eggs vs. eggs and dead bodies).
16. Dry plate in sterile hood, wrap in parafilm, and place in incubator to hatch overnight.

Nematode Growth Media (NGM) Plate Protocol

1. Add H20, NaCl, Peptone, and Agar using the attached plate recipes to the appropriate size bottle (do not autoclave bottles more than half full). Add stir bar and mix on stir plate until dissolved.
2. Autoclave on liquid 30 or liquid 45 setting depending on the amount of liquid being autoclaved. The cap MUST be loose. Make sure to add a piece of autoclave tape onto the bottle before autoclaving.

3. Place the bottle on a hot plate at ~75 degrees with stirring to keep the media at the correct temperature until you are ready to pour. When ready to pour, the media temperature should be at ~55C (you should be able to hold your hand on the bottle for 5-10 seconds without it being too hot).
4. Add the MgSO4, CaCl2, cholesterol, KH2PO4, and any additional antibiotics using the attached recipes and stir on hot plate.
5. Pipette out 25 ml of the media onto 100mm plates or 10 ml of media onto 60mm plates.
6. Allow to dry overnight at room temperature on the bench before seeding.
7. To seed, add 200 ml of the appropriate bacteria culture to the 100mm plates or 100 ml to the 60mm plates.
8. Spread bacteria using the metal spreader and allow the bacteria to dry overnight at room temperature on the bench.
9. Place the plates in a plastic container or tied and sealed with tape into the plastic sleeve the plates come in. Place them in the 4C fridge/cold room for storage (Plates can be stored at 4C for approximately 1 month).

NGM Plates

# of 100mm Plates	**8**	**16**	**24**	**32**	**40**
H_20 (mL)	200	400	600	800	1000
NaCl (g)	0.6	1.2	1.8	2.4	3
Peptone (g)	0.5	1	1.5	2	2.5
Agar (g)	3.4	6.8	10.2	13.6	17
Add stir bar and autoclave					
Cool to 55°C then aseptically add:					
$MgSO_4$ (µL)	200	400	600	800	1000
$CaCl_2$ (µL)	200	400	600	800	1000
Cholesterol (µL)	200	400	600	800	1000
KH_2PO_4 (mL)	5	10	15	20	25

OP50-1 Plates

# of 100mm Plates	**8**	**16**	**24**	**32**	**40**
H_20 (mL)	200	400	600	800	1000
NaCl (g)	0.6	1.2	1.8	2.4	3
Peptone (g)	0.5	1	1.5	2	2.5
Agar (g)	3.4	6.8	10.2	13.6	17
Add stir bar and autoclave					
Cool to 55°C then aseptically add:					
$MgSO_4$ (µL)	200	400	600	800	1000
$CaCl_2$ (µL)	200	400	600	800	1000
Cholesterol (µL)	200	400	600	800	1000
KH_2PO_4 (mL)	5	10	15	20	25
Streptomycin (uL)	200	400	600	800	1000

NA22 Plates

# of 100mm Plates	**8**	**16**	**24**	**32**	**40**
H_20 (mL)	200	400	600	800	1000
NaCl (g)	0.24	0.48	0.72	0.96	1.2
Peptone (g)	4	8	12	16	20
Agar (g)	5	10	15	20	25
Add stir bar and autoclave					
Cool to 55°C then aseptically add:					
$MgSO_4$ (µL)	200	400	600	800	1000
$CaCl_2$ (µL)	200	400	600	800	1000
Cholesterol (µL)	200	400	600	800	1000
KH_2PO_4 (mL)	5	10	15	20	25

RNAi Plates

# of 100mm Plates	**8**	**16**	**24**	**32**	**40**
H_20 (mL)	200	400	600	800	1000
NaCl (g)	0.6	1.2	1.8	2.4	3
Peptone (g)	0.5	1	1.5	2	2.5
Agar (g)	3.4	6.8	10.2	13.6	17
Add stir bar and autoclave					
Cool to 55°C then aseptically add:					
$MgSO_4$ (µL)	200	400	600	800	1000
$CaCl_2$ (µL)	200	400	600	800	1000
Cholesterol (µL)	200	400	600	800	1000
Carb (µL)	200	400	600	800	1000
IPTG (µL)	200	400	600	800	1000
OR 20% Lactose (mL)	2	4	6	8	10
KH_2PO_4 (mL)	5	10	15	20	25

Worm Picking

1. Sterilize the metal pick using a flame and keep the flame near the microscope to prevent airborne contamination.
2. Pick up a small amount of bacteria onto your pick and use the sticking or scooping method to pick up the worm and transfer it from one plate to another.
3. Do not allow a worm to sit on the pick for more than 30-60 secs or it will dry up and die. Be very gentle when using the metal pick as to not damage the worm during the process.
4. Gently place the worm on the new plate, being careful not to dig into the agar. Placing the worm outside of the bacteria lawn and straight on the agar makes it easier to remove the worm off of the pick.
5. Re-flame the pick periodically to remove excess bacteria and prevent contamination. Always re-flame pick after each strain to prevent cross contaminating your worm strains.

6. If using a hair pick, spray or dip the pick in ethanol to clean (it will never be perfectly sterile) and use it to transfer worms.
7. Note: Every pick behaves differently, and you will need to play around with your own personal picking technique. Practice, practice, practice.

Worm Chunking

1. Take out fresh plate (OP50 or NA22) to warm up to room temperature.
2. Light Bunsen burner and wear gloves.
3. Spray metal spatula with 70% ethanol and pass-through flame 3-4 times to sterilize the end. Allow spatula to cool for 10-15 seconds.
4. Cut out a small 1 cm cube of agar from the source plate and transfer it “worm side” down to the new plate.
5. Use the spatula to scrape the worm side of the chunk across the plate to spread out the worms.
6. Observe under the microscope for worms on the new plate, rechunk if none are seen or all worms are dead.
7. Wrap plate with parafilm and place in incubator.
8. Note: Chunking is a non-sterile procedure so if your source plate is heavily contaminated, the new plate will also become contaminated. If the worms are particularly sick you may want to consider doing a bleach prep in the future to clean the strain up.

Worm Freezing

1. Bring freezing chamber to room temp and ensure it is appropriately filled with isopropyl alcohol.
2. Prepare 5 replicate cryovials per strain you wish to freeze. On the side of each cryovial, label it with the strain name, date frozen, your initials, and tube # (ex. 1/5, 2/5, 3/5, etc). On the top of each tube, label with just the strain name.
3. Allow an OP50 plate to completely starve out. Ideally, you'll end up with a population consisting of ~10-20,000 of starving L1 and L2 animals with a few adults. Older worms do not survive the freezing process well.
    a. Note: If plates are heavily contaminated, bleach and allow to restarve.
4. Chunk some of each strain to a fresh OP50 plate in case the freezing recovery goes poorly.
5. Wash the rest of each plate into a 15 ml tube with NGM buffer.
6. Repeat wash step until supernatant becomes clear. And then remove supernatant leaving 2.5 ml of NGM in tube.
7. Add 2.5 ml worms freezing media and mix thoroughly.
8. Resuspend worms evenly using the pipet, then pipet 1 ml into each of the cyrovials.
9. Place all cryovials to be frozen in the freezing chamber and immediately place in -80C.

Worm Thawing

1. Remove cryovial of your strain of interest. Hold the tube in your hand to quickly warm it up.

2. In the sterile hood, once thawed, mix the tube carefully and pipet the worms onto OP50 plates.
3. Let the plates dry completely, wrap with parafilm and place in worm incubator.
4. The next day check the thaw plate for the number of live worms. Estimate the recovery rate of each strain frozen (good, ok, excellent, etc.).
5. If thaw did not work well, regrow strain and try again. Remember to remove worms from thawed plate after 2-3 days of recovery.
6. If the thawed cryovial is the last freezer stock of the strain, follow the worm freezing protocol to freeze more to ensure there is always freezer stocks for each strain.

Thrashing/Mobility Assay

1. Synchronize worms in one of the following ways:
    a. Bleach synchronization
    b. Pick the desired number of L4-stage worms to an OP50 plate.
2. Once synchronized worms have reached adulthood, pick an individual worm into a 6-8 uL drop of M9/NGM buffer on a glass slide.
3. Allow the worms to recover from the transfer for 1 minute, and then count the number of thrashing movements in 30 seconds under the microscope.
4. Repeat steps 2 and 3 for all worms in the trial (~15-20).

Thermotolerance

1. Synchronize worms using bleach protocol and grow worms to Day 1 of adulthood.

2. On Day 1 of adulthood, place plates in 37C incubator or in 37C water bath (ensure plate is properly parafilmed to prevent water leakage into plate) for 3.5 hours.
    a. Note: The heat shock conditions can be optimized for each specific experiment and worm age. The goal is to find an optimal temperature and incubating time that yields ~50% survival rate under control conditions. That way you can visualize both increases and decreases in thermotolerance ability in your experimental samples.
3. Remove plates from heat shock and place in 20C incubator for 24 hours to allow for recovery.
    a. Note: Recovery time can also be optimized for each experiment. I have done 24–48-hour recoveries.
4. After recovery period, randomly score 100 worms from around the entire plate and gently poke with pick to determine if the worm is alive or dead.
    a. Note: Ensure you are evenly scoring worms around the entire plate to ensure random selection. I survey 100 random worms on a plate of 1000s, however you can also only plate ~100 worms onto your plate after synchronizing and score all worms.
5. Calculate survivability from alive/dead ratio and graph.

Lifespan Assay

1. Synchronize worms by following the beach protocol and plate L1-arrested worms on an OP50 plate.
2. Allow worms to develop at 20C for 1-2 days, or until they reach the L4 stage.

3. Passage ~50 L4 worms to RNAi plates.
4. Passage each worm to a new RNAi plate for the first 5 days of adulthood (gravidity period), determining their status by observing movement and/or poking them with a sterilized poker. Worms that do not respond to repeated poking are considered dead.
5. Dispose of deceased worms and record the number of dead, alive and censored worms. Worms that are "bagged", have vulva protrusions, etc are censored.
6. Repeat steps 4-5 until all worms have died.

Generating Males

1. Set up ~4 OP50 plates containing 10 L4 hermaphrodites each.
2. Heat shock 4 hours at 33C.
3. Move plates to 20C. You should get a few males in the F1 generation.
4. Maintain the male stocks by plating 9 males and 3 L4 hermaphrodites on a crossing plate (NGM plate with agarose instead of agar, added streptomycin, and 8 ul of OP50-1 culture).

Genetic Cross Protocol

1. Plate 9 N2 males and 3 2nd strain L4 hermaphrodites onto a plate with a small dot of OP50. Allow the worms to mate and grow progeny to L4/adulthood (~3-5 days). Half of the progeny should be male.

2. Pick 9 progeny males to a new OP50 plate. Add 2 3rd strain L4 hermaphrodites. Allow the worms to mate and grow progeny to L4/adulthood (~3-5 days). Half of the progeny should be male.
3. There is a 1/32 chance of finding a worm homozygous for both genes from the two strains. Pick ~40 hermaphrodite progeny onto individual plates. Allow worms to self-fertilize and grow progeny to L4/adulthood (~3-5 days).
4. NOTE: If all the progeny has the phenotype you're looking for, you know the mom is homozygous. If only ~75% have the phenotype, you know the mom is heterozygous.
5. Use assays specific for each strain of interest to determine if the progeny contain your genes of interest.
    a. For example, if one of your strains contains a roller phenotype, examine your cross for worms with a roller phenotype. If every single worm is a roller, then you know the mom is homozygous for that phenotype. If only 75% have the phenotype, they are heterozygous. If that's the case, pick progeny to individual plates and allow to self-fertilize. If all of their progeny has the phenotype then the mom was homozygous for both genes.
6. Utilize Punnett square genetics to determine phenotype ratios for each gene of interest. The goal is to obtain a worm that is homozygous for both genes from each strain.

RNA Extraction

NOTES:

- Always pipet Trizol in the fume hood and dispose in liquid/solid waste

- Always use filter tips
- Spray bench, pipettors, and gloves with 70% EtOH and then RNAse away prior to starting
- Keep everything on ice or at 4C as much as possible
- Discard all solid waste into biohazardous waste

1. Pick 30-35 worms into 20 ul of NGM in 1.5mL tubes and place tubes immediately on ice.
2. In the fume hood, add 250 ul of Trizol to each tube (Tri-reagent in 4C fridge).
3. Sonicate samples:
    a. BioRuptor sonicator: 30 sec ON, 30 sec OFF 10x on ice.
    b. Handheld sonicator: setting 2-3 twice for 12 seconds each.
4. Add 250 ul of 100% ethanol to samples and vortex for 10 seconds.
5. Load mixture into a spin column and centrifuge at max speed for 1 min at 4C.
6. Transfer spin column to new collection tube and pour flow through in 15mL tube of hazardous waste. Discard old collection tube in hazardous waste.
7. Add 400 ul Direct-zol RNA prewash to column, centrifuge at max speed for 1 minute at 4C, discard flow through. Repeat this step one more time.
8. Add 700 ul RNA wash buffer to column, centrifuge at max speed for 1 minute at 4C, and discard flow through.
9. Spin column for 2 minutes to dry column.
10. Place spin column into new DNAse/RNAse free 1.5mL tube.
11. Add 10-20ul RNAse-free water to column filter, let sit for 1 minute at room temperature, centrifuge at max speed to elute RNA at 4C.

12. Add another 10-20ul RNAse-free water to elute more RNA, let sit for 1 minute at room temperature, centrifuge at max speed to elute RNA at 4C.
13. Nanodrop samples.

Optional in-column DNAse treatment:

1. After step 10 wash the column with 400 ul of RNA wash buffer, centrifuge for 1 min, discard flow-through.
2. Prepare DNase 1 reaction mix as follows, recipe is given for 1 sample, make a mastermix for as many samples as you have.
    a. RNA wash buffer – 64 ul
    b. Nuclease free H20 – 3 ul
    c. 10x DNase 1 reaction buffer – 8 ul
    d. DNAse 1 – 5 ul
3. Add 80 ul DNase 1 reaction mix directly to column filter. Incubate at RT for 15 min centrifuge for 1 min.
4. Continue with step 11.

qPCR Protocol

1. Thaw reagents then place on ice; invert SYBR green gently to mix.
2. Make your target and control master mixes (MM) using the SYBR green general protocol (+10% extra) or the lab's qPCR setup excel sheet, then quickly vortex and spin down.
3. Distribute 62.7 ul of the MM to 1.5 mL tubes (as many tubes as cDNA samples to be tested for each master mix).

4. Make the cDNA dilutions from the excel sheet in 0.625 mL tubes.
5. Add 3.3 uL of cDNA dilutions to the 1.5 mL tubes, then quickly vortex and spin down.
6. Pipet 20 ul of completed MM+cDNA to qPCR plate wells in triplicate.
7. Seal plate with optical tape and run reaction.
8. Computer steps:
    a. Turn on machine and open StepOne software once it finished starting up.
    b. Click the arrow next to “New Experiment” and choose “Advanced Setup”.
    c. Name the experiment.
    d. Click:
        i. StepOne Plus Instrument (96 wells)
        ii. Quantitation – comparative Ct(ΔΔCt)
        iii. SYBR green reagent
        iv. Standard (~2 hrs to complete a run)
    e. Click “Plate Setup” on the left and add your target and sample names on the “Define targets and samples” tab.
    f. Click to the “Assign targets and samples” tab to assign them to the correct wells.
    g. Click start run.

APPENDIX D: COPYRIGHT PERMISSIONS

Copyright permissions statement for Chapter Two: